



Title	LC/MS analysis of storage-induced plasmalogen loss in ready-to-eat fish
Author(s)	Chen, Zhen; Jia, Jiaping; Wu, Yue et al.
Citation	Food Chemistry, 383, 132320 <a href="https://doi.org/10.1016/j.foodchem.2022.132320">https://doi.org/10.1016/j.foodchem.2022.132320</a>
Issue Date	2022-07-30
Doc URL	<a href="https://hdl.handle.net/2115/90206">https://hdl.handle.net/2115/90206</a>
Rights	© 2022. This manuscript version is made available under the CC-BY-NC-ND 4.0 license <a href="http://creativecommons.org/licenses/by-nc-nd/4.0/">http://creativecommons.org/licenses/by-nc-nd/4.0/</a>
Rights(URL)	<a href="https://creativecommons.org/licenses/by-nc-nd/4.0/">https://creativecommons.org/licenses/by-nc-nd/4.0/</a>
Type	journal article
File Information	Chen202207.pdf





16 **Abstract**

17 Plasmalogens are functional and oxidation-sensitive phospholipids abundant in fish. Chilling  
18 and freezing are common storage methods for maintaining the quality of fish, but their effect  
19 on plasmalogen preservation has not been studied. Therefore, plasmalogen loss in ready-to-  
20 eat tuna meat during storage under different conditions was investigated. LC/MS was used to  
21 analyze the time- and temperature-dependent changes of plasmalogens, which was the most  
22 evident for the species with an ethanolamine headgroup and polyunsaturated fatty acyl  
23 chains. Moreover, a series of oxidized plasmalogen molecules were identified, and their  
24 storage-induced accumulation was observed. Plasmalogen loss was strongly correlated with  
25 total lipid oxidation and phospholipid degradation. Repeated freeze-thaw cycles were found  
26 to accelerate the loss of plasmalogens, whereas the different thawing methods did not. The  
27 present study provides a deeper understanding of changes in lipid nutrients from fish meat  
28 during storage and demonstrates the importance of using advanced strategies to maintain food  
29 quality.

30

31 **Keywords**

32 Dietary phospholipids; tuna meat; plasmalogen oxidation; lysophospholipids; freeze-thaw  
33 cycles.

## 34 **1. Introduction**

35 Plasmalogens are a kind of dietary phospholipids with various beneficial effects, such as anti-  
36 oxidation (Wu et al., 2019), anti-inflammation (Sejimo et al., 2018), anti-atherosclerosis  
37 (Ding et al., 2020), and neuronal protection (Yamashita et al., 2016). Their molecular  
38 structures consist of a vinyl-ether-linked chain, an ester-linked fatty acyl chain, and a  
39 phosphate headgroup at the *sn*-1, *sn*-2, and *sn*-3 positions of the glycerol backbone,  
40 respectively. Depending on the headgroup, plasmalogens are classified into two main types:  
41 choline plasmalogen (PlsCho) and ethanolamine plasmalogen (PlsEtn) (Figure 1A).

42 It is widely believed that intake of bioactive lipids is beneficial for maintaining health,  
43 preventing some diseases, and treating certain illnesses. Therefore, the evaluation of quality  
44 and quantity of these lipids in foods has gained the attention of scientists. Fish is a well-  
45 known source of essential lipids, particularly the major dietary polyunsaturated fatty acyls  
46 (PUFA). Plasmalogens are recognized as a “storage pool” of PUFA because their *sn*-2 group  
47 is usually a PUFA (J. Wang et al., 2021). PUFA-rich plasmalogens are abundant in aquatic  
48 animal food-products, including food-products from fish and shellfish (Wu et al., 2021).  
49 Hence, these seafoods have been proposed to help prevent cardiovascular disease and  
50 metabolic disorders, e.g., atherosclerosis, nonalcoholic steatohepatitis, and Alzheimer’s  
51 disease (Ding et al., 2020; Jang et al., 2017; Su et al., 2019).

52 It is vital to ensure the quality and freshness of fish due to its highly perishable nature.  
53 This is particularly the case for ready-to-eat raw fish dishes, such as sushi and sashimi in

54 Japan and gravlax in Nordic countries. Therefore, after catching, fish are usually kept  
55 refrigerated or frozen to extend their shelf-life and increase market accessibility. However,  
56 these storage methods induce some changes in the quality of fish, such as color, texture,  
57 flavor, and microbial profile (Coombs et al., 2017; Soyer et al., 2010). In terms of chemical  
58 components, researchers have demonstrated that the denaturation, rancidity, degradation, and  
59 oxidation of proteins and lipids are mainly responsible for the decline in quality and  
60 nutritional value of foods (Aguilera Barraza et al., 2015). These changes are exacerbated by  
61 inappropriate thawing methods and excessive freeze-thaw cycles (Ali et al., 2015; B. Wang et  
62 al., 2020).

63 Compared with that of conventional evaluation methods, better food quality control can be  
64 achieved using the recently proposed “food fingerprinting” strategy that employs an omics  
65 approach (Medina et al., 2019). The quality change in fish during storage has been analyzed  
66 on the basis of proteins, enzymes, organic acids, biogenic amines, and volatile bases  
67 (Prabhakar et al., 2020). In contrast, studies on the lipidome changes remain quite limited.  
68 Especially, plasmalogens should be investigated at the molecular level, in order to precisely  
69 monitor their easily neglected quality changes and assess the variation in related nutrients. In  
70 our previous study, we discovered that plasmalogens were significantly reduced during high-  
71 temperature cooking processes (Wu et al., 2020). Although such an issue does not exist for  
72 ready-to-eat raw fish, the loss of plasmalogens during preservation remains unknown.

73 Based on the above considerations, the present study aimed to clarify changes in

74 plasmalogens in ready-to-eat raw fish meat during storage using liquid chromatography-mass  
75 spectrometry (LC/MS). Detailed variations of plasmalogen species with different headgroups  
76 (PlsCho and PlsEtn) and various fatty acyls were semi-quantitatively characterized during  
77 freezing and chilling under different conditions. The influences of common thawing methods  
78 and the number of freeze-thaw cycles were also evaluated and discussed.

79

## 80 **2. Materials and methods**

### 81 **2.1. Chemicals**

82 Chloroform, methanol, isopropanol, and water of spectral grade were purchased from Sigma-  
83 Aldrich (St. Louis, USA). The plasmalogen standards PlsCho p16:0/17:0 and  
84 PlsEtn p16:0/17:0 were chemically synthesized (Wu et al., 2020), while other lipid standards  
85 were obtained from Avanti Polar Lipids (Alabaster, USA) and Sigma-Aldrich. A mixed  
86 solution containing all internal standards was prepared with methanol and stored at  $-80\text{ }^{\circ}\text{C}$   
87 until use, and the concentration of each standard in the mixture is listed in Table S1. Unless  
88 otherwise specified, other chemical reagents were of analytical grade and acquired from  
89 Kanto Chemical Co., Inc. (Tokyo, Japan).

### 90 **2.2. Sample preparation**

91 Fresh lean tuna meat was purchased from a local provider in Sapporo, Japan, of which the  
92 fish were harvested in Hokkaido, Japan. The samples were kept on ice and transported  
93 immediately to the laboratory within 20 min. Upon arrival, the samples were cut into uniform

94 pieces of 4 cm × 4 cm × 2 cm and packaged in polyethylene bags. Unless specified otherwise,  
95 fresh tuna meat was designated as the “control sample,” which was used to measure the  
96 baseline lipid levels. In all subsequent experiments, the samples were analyzed in  
97 quadruplicates (unless specified otherwise).

### 98 **2.2.1. Freezing and chilling conditions**

99 Frozen tuna samples were stored at −25 °C, −40 °C, or −80 °C for up to 90 days, and lipid  
100 extraction was performed at 1, 2, 3, 4, 5, 6, 7, 10, 15, 30, 45, 60, and 90 days. The chilled  
101 samples were stored at 4 °C for up to 15 days, and lipid extraction was performed at 1, 2, 3,  
102 4, 5, 6, 7, 10, and 15 days. The frozen samples were subsequently used for lipid extraction.

### 103 **2.2.2. Thawing methods**

104 Four commonly used thawing methods were compared: refrigerator thawing (RT, 4 °C), air  
105 thawing (AT, 20 °C), water immersion thawing (WT, 18 °C), and microwave thawing (MT,  
106 200 W). Fresh samples were frozen at −25 °C for 3 days and then thawed using one of the  
107 four methods, till the core temperature reached 4 °C (B. Wang et al., 2020). The required  
108 thawing times were: 3 h for RT, 1.5 h for AT, 25 min for WT, and 1 min for MT. The control  
109 samples were analyzed directly without thawing.

### 110 **2.2.3. Freeze-thaw cycles**

111 In each freeze-thaw cycle, the sample was frozen at −25 °C for 21 h and then thawed at 4 °C  
112 for 3 h. This treatment was repeated for up to 7 cycles. In these experiments, the control  
113 samples were the fresh ones (without freezing or thawing) and those kept frozen for 1 to 7

114 days (without thawing).

### 115 **2.3. Lipid extraction**

116 Lipid extraction was carried out according to Folch et al. (Folch et al., 1957) with some  
117 modifications (Wu et al., 2020). Briefly, the tuna meat sample was directly homogenized  
118 using a kitchen homogenizer (Joyoung Co., Ltd., Hangzhou, China). Then, approximately  
119 50 mg of the homogenized sample was placed in a 1.5 mL Eppendorf® tube and weighed  
120 precisely. The homogenate was extracted twice with 900 µL of ice-cold solvent that consisted  
121 of chloroform/methanol in 2:1 (v/v) with 0.002% butylated hydroxytoluene and internal  
122 standards (for the amount of each internal standard see Table S1). This was followed by  
123 vacuum concentration, dissolution of extracts in methanol, and filtration to remove any  
124 residue. The whole lipid extraction procedure was completed within 1 h to minimize lipid  
125 oxidation or degradation, and the prepared lipid extracts were kept at –80 °C until LC/MS  
126 injection.

### 127 **2.4. LC/MS analysis**

128 The determination of plasmalogens and other lipids was performed using a Shimadzu  
129 Prominence HPLC (Shimadzu Corp., Kyoto, Japan) coupled to an LTQ Orbitrap MS  
130 (Thermo-Fisher Scientific Inc., San Jose, CA, USA). The chromatographic conditions were  
131 as follows: Atlantis T3 C18 column (2.1 mm × 150 mm, 3 µm, Waters, Milford, MA, USA),  
132 oven temperature of 40 °C, and flow rate of 200 µL/min. The mobile phases were as follows:  
133 10 mM aqueous ammonium acetate (A), isopropanol (B), and methanol (C). The elution

134 gradient was as follows: 0–1 min, 40%A+20%B+40%C; 1–5 min, 20%A+50%B+30%C; 5–  
135 12 min, 5%A+70%B+25%C; 12–28 min, 3%A+82%B+15%C; 28–36.5 min,  
136 3%A+85%B+12%C; 36.5–37.5 min, returned to the initial condition, followed by 40 min for  
137 re-equilibration. For MS detection, the following parameters were applied for both  
138 electrospray ionization (ESI)-positive and ESI-negative modes: spray voltage of 3 kV,  
139 capillary temperature of 330 °C, and Fourier transform mode resolution power of 30 000. The  
140 scanning parameters were based on our previous study (Wu et al., 2020): the high-resolution  
141 (HR) MS<sup>1</sup> data were obtained in the range of *m/z* 250–1100 for ESI-positive mode and in  
142 *m/z* 220–1650 for ESI-negative mode, while the tandem MS data were acquired using  
143 collision-induced dissociation (CID). The collision energy values for MS<sup>2</sup>, MS<sup>3</sup>, and MS<sup>4</sup>  
144 were set at 35.0, 40.0, and 40.0, respectively.

145 The raw data were processed using the workstation Xcalibur 2.3 (Thermo-Fisher Scientific  
146 Inc.). The annotation of plasmalogens and other lipids was based on the retention behavior  
147 and HR-MS signals with a tolerance of 5.0 ppm. The annotated lipids were labeled as “lipid  
148 class + the number of acyl carbon atoms + the number of acyl double bonds.” The fatty acyl  
149 composition of the intact lipid molecular species was determined with the help of MS/MS  
150 fragmentation, which was based on comparison with LIPIDMAPS ([www.lipidmaps.org](http://www.lipidmaps.org)) and  
151 our in-house library (Z. Chen et al., 2020; Wu et al., 2019, 2020). The semi-quantitation of  
152 plasmalogens and other unoxidized lipids was based on the extracted ion chromatogram  
153 (EIC) peak areas of the analyte and the IS, according to the following equation:

154 
$$Amount_{analyte} = \frac{Peak\ area_{analyte}}{Peak\ area_{internal\ standard}} \times Amount_{internal\ standard}$$

155 Because we lacked internal standards for oxidized lipids, their semi-quantitative  
156 measurement was based on calculating the peak area as the analyte intensity.

157

## 158 **2.5. Measurement of thiobarbituric acid-reactive substances (TBARS) content**

159 TBARS level was measured according to previous studies (Jiang et al., 2019; Li et al., 2019)  
160 with some modifications. In brief, 100 mg homogenized sample was mixed with 1 mL acetic  
161 acid solution (pH = 4.0, adjusted by NaOH) containing 0.1% EDTA, followed by  
162 centrifugation (5000 rpm, 20 min, 4 °C) to obtain the supernatant. Next, 200 µL of the  
163 supernatant was reacted with 1 mL of 20 mM thiobarbituric acid (TBA) at 100 °C for 1 h.  
164 The reaction was terminated by cooling in an ice bath for 10 min, and then the mixture was  
165 separated by centrifugation at 12 000 rpm for 10 min at 4 °C. Fluorescence of the final  
166 supernatant was measured at 532 nm using a spectrofluorometer (FP-6500, JASCO, Tokyo,  
167 Japan). Malonaldehyde (MDA) prepared from 1,1,3,3-tetraethoxypropane (TEP) was used to  
168 obtain the TBARS calibration curve, and the TBARS values were expressed in units of  
169 mg MDA/kg sample.

## 170 **2.6. Statistical analysis**

171 All results were expressed as mean ± standard deviation (SD). Two-tailed Student's t-test and  
172 one-way ANOVA (using Tukey's post hoc test) were carried out using GraphPad Prism 8 (La  
173 Jolla, CA, USA).  $P < 0.05$  was considered significantly different. Correlation analysis and the

174 following heatmap illustration were performed using R 4.1 (R Core Team, 2021). Principal  
175 component analysis (PCA) and artificial neural network (ANN) modeling were conducted  
176 using JMP 16 pro (SAS Institute Inc., Cary, NC, USA).

177

### 178 **3. Results and discussion**

#### 179 **3.1. Time- and temperature-dependent loss of plasmalogens during storage**

##### 180 **3.1.1. Decrease in the content of total plasmalogens**

181 Representative photographs of tuna meat samples during storage by freezing/chilling are  
182 shown in Figure 1B. The content of total plasmalogens, defined as the sum of all the detected  
183 intact plasmalogen species (for the identification details see Table S2), was compared at  
184 different storage times and temperatures. As shown in Figure 1C, approximately 90% of the  
185 total plasmalogens was retained after 90 days of frozen storage under  $-40\text{ }^{\circ}\text{C}$  and  $-80\text{ }^{\circ}\text{C}$ .  
186 Samples frozen under  $-25\text{ }^{\circ}\text{C}$  showed a slight decrease ( $94.5\% \pm 2.0\%$  of control) in  
187 plasmalogen content within the first 5 days, followed by an obvious decline toward the end to  
188 reach  $68.7\% \pm 1.9\%$  of the control (i.e., fresh samples without freezing or chilling). Chilling  
189 at  $4\text{ }^{\circ}\text{C}$  did not preserve the plasmalogens well, since their total amount was only  
190  $53.8\% \pm 2.2\%$  after 15 days. Similar results have been reported for the loss of other fat-  
191 soluble nutrients (e.g., fatty acids and certain vitamins) during long-term storage (Karlsdottir  
192 et al., 2014; Santos et al., 2012; Zhou et al., 2019). A major issue is temperature variation,  
193 which is associated with physiological and biochemical changes in lean meat as well as

194 microbial activity (Ali et al., 2015).

### 195 **3.1.2. Variation in characteristics of plasmalogen fingerprints**

196 Because plasmalogens include many molecular species, storage-induced variations in their  
197 profile need comprehensive investigation. To obtain a general overview, we conducted PCA  
198 using the plasmalogen molecular composition as variables for all the samples. There were a  
199 total of 198 samples: 52 for each group frozen under  $-25\text{ }^{\circ}\text{C}$ ,  $-40\text{ }^{\circ}\text{C}$ , or  $-80\text{ }^{\circ}\text{C}$ ; 36 for the  
200 group chilled at  $4\text{ }^{\circ}\text{C}$ ; and 6 for the control group (not frozen or chilled). Most of the variance  
201 was adequately explained by the first two principal components (50.6% and 12.3% of the  
202 total explained variance). Separate score plots for each storage temperature (Figure 2A) show  
203 time- and temperature-dependent clustering. All samples frozen under  $-40\text{ }^{\circ}\text{C}$  and  $-80\text{ }^{\circ}\text{C}$   
204 were grouped tightly; those frozen under  $-25\text{ }^{\circ}\text{C}$  were loosely grouped and showed  
205 noticeable divergence after 10 days. Samples chilled under  $4\text{ }^{\circ}\text{C}$  displayed migration toward  
206 the positive x-axis, which corresponded with storage time from day 4 onward, moving  
207 gradually away from the control. These data suggest that a higher storage temperature  
208 (particularly chilling at  $4\text{ }^{\circ}\text{C}$ ) causes more changes in the plasmalogen fingerprint.

209 Figure 2B compares the two plasmalogen types, namely PlsCho and PlsEtn with different  
210 headgroups. Both exhibited a decreasing trend during storage. PlsEtn was more unstable than  
211 PlsCho under all investigated temperatures, and their difference was especially obvious at  
212 higher temperatures. Consistently, in case of the corresponding diacyl glycerophospholipids,  
213 the amount of phosphatidylethanolamine (PE) remained significantly lower than that of

214 phosphatidylcholine (PC). Similar studies claimed that PE was more susceptible to hydrolysis  
215 or oxidation than PC during the dry curing of meat (Pérez-Palacios et al., 2010; Xu et al.,  
216 2008). The present results also suggest the parallel explanation that plasmalogens containing  
217 ethanolamine (PlsEtn) suffer more loss during storage than those containing choline  
218 (PlsCho).

219 Interestingly, PlsEtn (with a vinyl-ether linkage at *sn*-1) experienced less loss than PE  
220 (with an ester linkage at *sn*-1) when stored under  $-25\text{ }^{\circ}\text{C}$  and  $4\text{ }^{\circ}\text{C}$ , even though they share  
221 the same headgroup. In contrast, such phenomenon was not found under  $-40\text{ }^{\circ}\text{C}$  or  $-80\text{ }^{\circ}\text{C}$   
222 (Figure 2B). One possible explanation is that at higher storage temperatures, phospholipids  
223 were partially hydrolyzed by active enzymes, such as lipases and phospholipases (Qinsheng  
224 Chen et al., 2017), and more ester linkages mean easier enzymatic reactions. However, such  
225 difference according to the linkage was not observed between PlsCho and PC. These results  
226 seem to contradict the conventional view that the vinyl-ether linkage serves as a sacrificial  
227 antioxidant functional group (Broniec et al., 2011; Morel et al., 2021). Whether there are  
228 specific mechanisms that stabilize plasmalogens and how they work are worthy questions for  
229 future investigations.

230 Figure 2C compares the fatty acyl compositions across the samples. The levels of PUFAs  
231 such as C22:6 and C20:5 were sharply depleted when stored for longer times and under  
232 higher temperatures. It is noted that there were higher PUFA levels in PlsEtn than in PlsCho  
233 (e.g.,  $68.5\% \pm 0.8\%$  vs.  $23.6\% \pm 1.0\%$  for C22:6,  $P < 0.001$ ), which might explain the

234 different stabilities of PlsEtn and PlsCho (Pérez-Palacios et al., 2010; Xu et al., 2008).

235 According to these results, the stability of plasmalogen species depends on both the

236 headgroup and the fatty acyl at the *sn*-2 position.

## 237 **3.2. Potential mechanisms of plasmalogen loss during storage**

### 238 **3.2.1. Identification of oxidized plasmalogens**

239 Since plasmalogens are easily oxidizable food nutrients, we were interested to know whether

240 and how they become oxidized during long-term storage, as well as the possible connection

241 between oxidation and plasmalogen loss. To the best of our knowledge, there have been no

242 available libraries for oxidized plasmalogens so far. Therefore, first, we identified a series of

243 oxidized plasmalogen molecules as the oxidation products based on HR-MS signals and

244 tandem MS fragmentation characteristics (Table S3). For instance, the HR-MS<sup>1</sup> data in

245 Figure 3A indicate a signal at *m/z* 810.4937 that corresponds to C<sub>43</sub>H<sub>74</sub>O<sub>11</sub>NP<sup>-</sup> (calculated

246 *m/z*: 810.4927, Δppm = 1.23). Considering both the formula (63.9797 Da greater than

247 PlsEtn 38:6) and the retention time (approximately 4 minutes shorter than PlsEtn 38:6) in the

248 corresponding EIC, we assumed the existence of oxidation product PlsEtn 38:6+4[O]. In the

249 following MS<sup>2</sup>, compared with that in the intact PlsEtn 38:6 (major fragments: *m/z* 436 as

250 loss of *sn*-2 acyl chain, *m/z* 327 as *sn*-2 RCOO<sup>-</sup> ion), there were three major extra ions,

251 namely *m/z* 452, *m/z* 391, and *m/z* 375, suggesting the addition of 1[O] (*m/z* 436 + 16), 4[O]

252 (*m/z* 327 + 64), and 3[O] (*m/z* 327 + 48), respectively. The following MS<sup>3</sup> of *m/z* 452 gave

253 subsequent fragments of *m/z* 391 and *m/z* 255, which were respectively assigned as

254  $[M - H - sn-2 \text{ acyl chain} - \text{ethanolamine}]^-$  and  $[sn-1 \text{ epoxy alcohol}]^-$  (or detached as  $\alpha$ -  
255 hydroxyaldehyde) based on the literature (Stadelmann-Ingrand et al., 2001; Weisser et al.,  
256 1997). The product ions of the  $m/z$  375 precursor ion exhibited continuous loss of  $H_2O$ ,  
257 suggesting one hydroxyl and one hydroperoxyl group. Therefore, one of the products in the  
258 mixture was speculated as PlsEtn p16:0(epo)/22:6(OH)(OOH). Similarly, the  $MS^3$  of  $m/z$  391  
259 and the  $MS^4$  further prompted the combination of two hydroxyl and one hydroperoxyl group.  
260 Thus, the other product of the isomer was disclosed as PlsEtn p16:0/22:6(OH)<sub>2</sub>(OOH).

261 Now, we further discuss the complexity of these oxidized plasmalogens. Taking the  
262 molecular species with fatty chain combination 38:6 (identified as p16:0/22:6) as an example,  
263 both PlsEtn and PlsCho were found with various oxidation degrees from +1[O] to +4[O],  
264 which were respectively classified as epoxides, hydroxides, and hydroperoxides according to  
265 the characterized MS fragmentation (Figure S1 – S8). Moreover, the fragment intensity  
266 differences indicated that the primary oxidation position for PlsEtn was the double bonds in  
267 the *sn*-2 fatty acyls ( $MS^2$  ion intensity:  $m/z$  436 >  $m/z$  452,  $m/z$  343 >  $m/z$  327; Figure S1),  
268 whereas for PlsCho it was easier to generate epoxy group on the vinyl-ether bond ( $MS^2$  ion  
269 intensity:  $m/z$  480 >  $m/z$  464,  $m/z$  327 >  $m/z$  343; Figure S5). When two or more oxygen  
270 atoms were added into the molecule, the *sn*-1/*sn*-2 +  $n[O]$  and the *sn*-1 + [O]/*sn*-2 + ( $n-1$ )[O]  
271 species were produced without selectivity. Possible reasons might include the proportion of  
272 PUFA in the *sn*-2 fatty acyls and the electrical charge on the headgroups.

273 **3.2.2. Oxidation and degradation as the potential mechanisms of plasmalogen loss**

274 Changes in oxidized plasmalogens were assessed for all samples (Figure 3B). The  
275 concentrations of both oxidized PlsEtn and oxidized PlsCho increased during storage. Among  
276 the four temperatures,  $-25\text{ }^{\circ}\text{C}$  produced the most drastic accumulation of all plasmalogen  
277 oxides, while  $-40\text{ }^{\circ}\text{C}$  resulted in much lower levels (only 0.3%–27.4% of that under  $-25\text{ }^{\circ}\text{C}$ ).  
278 Moreover, there was an even stronger relative reduction in the highly oxidized species at –  
279  $40\text{ }^{\circ}\text{C}$  (approximately 27% for both PlsEtn+1[O] and PlsCho+1[O], but less than 2% for  
280 PlsEtn+4[O] and PlsCho+4[O]). In addition, the plasmalogen oxides emerged at similar times  
281 under  $-25\text{ }^{\circ}\text{C}$  and  $-40\text{ }^{\circ}\text{C}$ : after 15 days for +1 [O] and after 30 days for +2 to +4 [O].  
282 Importantly, no oxidized plasmalogens were detected at any time in the samples kept under  
283  $-80\text{ }^{\circ}\text{C}$ . On the 15<sup>th</sup> day, the samples chilled under  $4\text{ }^{\circ}\text{C}$  showed higher levels of oxides than  
284 those kept under other temperatures. Also, the peak of oxidized plasmalogens first appeared  
285 in the chilled samples on the 7<sup>th</sup> day, suggesting that these unstable oxides produced under a  
286 relatively high temperature would undergo further reactions. The chain reactions of  
287 oxidation/peroxidation might affect other lipid components as well as the overall quality of  
288 the fish.

289 We also measured the levels of the oxidation products of other major lipid classes in the  
290 tuna meat samples, including triglycerides (TG), diglycerides (DG), free fatty acids (FFA),  
291 PC, and PE, according to our previously established LC/MS method (Z. Chen et al., 2020;  
292 Wu et al., 2019). The oxidation trends of these lipids were very similar to those of the

293 plasmalogen oxides (shown in Figure 4A). TG, DG, and FFA are known as the main lipid  
294 components of lean fish meat, while PC and PE are the major phospholipids. Therefore,  
295 oxidation of these lipids induces denaturation and rancidity, critically impacting the quality  
296 and nutritional value of the meat (Zhou et al., 2019). Meanwhile, we measured the TBARS  
297 levels in these samples (Figure 4A). As secondary products of lipid oxidation, TBARS were  
298 found to increase continuously during long-term storage, growing to 3.7-, 7.6-, 2.8-, and 1.2-  
299 fold of that of control under 4 °C, -25 °C, -40 °C, and -80 °C, respectively. These findings  
300 agree with the measured data for oxidized lipids.

301 Besides oxidation, degradation is another major pathway of plasmalogen loss in biological  
302 samples (Engelmann, 2004; Guang et al., 2010). Phospholipids are known to be hydrolyzed  
303 into lysophospholipids. For plasmalogens, the degradation products of PlsCho and PlsEtn are  
304 lysophosphatidylcholine (LPC) and lysophosphatidylethanolamine (LPE), respectively,  
305 together with FFA (Qinsheng Chen et al., 2017; Wu et al., 2019). Consequently, their levels  
306 were compared to the total amount of every molecular species within the same class  
307 (Figure 4B). Similar to the trend observed for oxidation products, the plasmalogen  
308 degradation products also accumulated in a temperature- and time-dependent manner.  
309 Notably, chilling (4 °C) for 15 days resulted in a larger amount of degradation products than  
310 that in all samples stored by freezing (up to 90 days). Lipid degeneration, which consists of  
311 oxidation and degradation, is considered the main limiting factor for the shelf-life of cold-  
312 stored fish (Tappi et al., 2020). According to our results, extended storage under 4 °C and

313 -25 °C caused significant degeneration of plasmalogens and other related lipids and storage  
314 under -40 °C could partially attenuate the degeneration, while storage under -80 °C could  
315 effectively inhibit such changes.

### 316 **3.2.3. Plasmalogen loss as an indicator of lipid degeneration and meat quality** 317 **deterioration**

318 To examine the possible use of plasmalogens as an indicator of fish quality, we analyzed the  
319 association between plasmalogen loss and other lipid degeneration indexes assessed in the  
320 current study. The Spearman's correlation coefficients were calculated for the samples stored  
321 under 4 °C and -25 °C, as summarized in the heatmap of Figure 5A. Significant positive  
322 correlations were observed for both temperatures (4 °C,  $r > 0.70$ ; -25 °C,  $r > 0.56$ ),  
323 suggesting an agreement between the reduction of intact plasmalogens and the accumulation  
324 of oxidized/degraded lipids. It was found that the total plasmalogens and PlsEtn levels  
325 correlated better to the lipid degeneration indexes than to PlsCho levels. Considering that  
326 TBARS are among the most common indicators of meat oxidation and quality deterioration,  
327 we made scatter plots of the TBARS levels and the loss rate of total plasmalogens for  
328 samples stored under all four temperatures (Figure 5B). The correlation coefficients were in  
329 the following order: -80 °C < -40 °C < -25 °C  $\approx$  4 °C, indicating that the plasmalogen loss  
330 was closely related to meat quality deterioration under commercial freezing and conventional  
331 chilling conditions. In addition, a higher storage temperature resulted in a steeper slope of the  
332 regression curve, suggesting that plasmalogens may be a more sensitive indicator of meat

333 quality than TBARS. Thus, the present work indicates the feasibility of a plasmalogen-based  
334 quality control strategy.

335 To provide a global view of plasmalogen loss during long-term storage, we established a  
336 non-linear prediction model based on ANN according to our previous method (Wu et al.,  
337 2020). ANN is a sophisticated simulation tool that can solve poorly understood problems in  
338 food science and technology (Ameer et al., 2017; Aung et al., 2022; Wu et al., 2020). The  
339 model was validated by comparing the fitted and measured values in both the training and the  
340 validation datasets (Figure S9). Figure 5C shows the predicted amounts of plasmalogens  
341 versus the storage temperature and storage time. A temperature between  $-40\text{ }^{\circ}\text{C}$  and  $-80\text{ }^{\circ}\text{C}$   
342 is sufficient for preserving the total content of plasmalogens and PlsEtn (with a retention of  
343 approximately 90% even after 90 days), while temperatures higher than  $-40\text{ }^{\circ}\text{C}$  are  
344 increasingly risky. In comparison, PlsCho was better preserved during storage: even after 30  
345 days under  $0\text{ }^{\circ}\text{C}$ , nearly 75% of PlsCho was present. Overall,  $-40\text{ }^{\circ}\text{C}$  appears to be a  
346 watershed temperature, which is in agreement with the results from a previous study that the  
347 state of water fraction and the properties of ice crystals under this optimum temperature were  
348 ideal for meat quality attributes (Leygonie et al., 2012). However, for conventional daily  
349 storage (chilling or freezing at approximately  $-20\text{ }^{\circ}\text{C}$ ), the content of intact plasmalogens was  
350 quite sensitive to the storage time and temperature. For instance, to preserve at least 60% of  
351 the total plasmalogens, the fish could be stored at above  $0\text{ }^{\circ}\text{C}$  for 11 days or frozen under  
352  $-10\text{ }^{\circ}\text{C}$  for up to 27 days. To keep more than 80% of the total plasmalogens, the storage times

353 are sharply shortened to 3 days and less than 6 days for 0 °C and -10 °C, respectively.  
354 However, if the freezing temperature is reduced to -20 °C, the storage limit could be  
355 extended to 14 days. The established model predicts a generally expected pattern, that a  
356 shorter storage time and a lower freezing temperature help preserve plasmalogens in stored  
357 tuna meat. Furthermore, the model could be a potential strategy for seafood suppliers and  
358 consumers to better predict and even control the food quality in terms of functional  
359 phospholipid nutrients.

### 360 **3.3. Effects of thawing on plasmalogen loss**

#### 361 **3.3.1. Different thawing methods had no effect on plasmalogens**

362 After freezing, the subsequent thawing process plays a critical role in the shelf-life of fish  
363 products (Ali et al., 2015). To explore the effects of thawing on plasmalogens, we measured  
364 the contents of total plasmalogens, PlsEtn, and PlsCho in samples thawed using the four  
365 common methods (Figure 6A). Compared to the sample without thawing, none of the thawed  
366 samples showed changes in the plasmalogen contents. It should be noted that the current  
367 results appear inconsistent with those of some previous studies, which demonstrated that  
368 various thawing methods affect the nutritional components (e.g., vitamins and polyphenols)  
369 and the degeneration indexes (e.g., TBARS and carbonyl content) (Holzwarth et al., 2012;  
370 Xia et al., 2012). This might be explained by the differences in the food samples, their  
371 chemical constituents, and the thawing conditions. Nevertheless, our results here suggest that  
372 none of the thawing methods caused noticeable plasmalogen loss during single thawing

373 process.

### 374 **3.3.2. Freeze-thaw cycles accelerate plasmalogen loss**

375 Repeated freeze-thaw cycles are known to accelerate the deterioration of food quality  
376 (Qingmin Chen et al., 2018). However, such results have not been reported for plasmalogens.  
377 The data in our present study indicated that plasmalogen loss became worse after multiple  
378 freeze-thaw cycles (Figure 6B). After two cycles, the total plasmalogen content was  
379 significantly reduced compared to that of the corresponding control ( $P < 0.01$ ), and the  
380 decline continued until the 7<sup>th</sup> cycle. At the end of 7 cycles, the freezing-only samples lost  
381 10.8% of the total plasmalogens, while those subjected to freeze-thaw cycles lost an extra  
382 12.4% ( $P < 0.001$  vs. freezing-only samples). PlsEtn exhibited a similar behavior with a  
383 higher loss than the freezing-only sample starting at the 2<sup>nd</sup> cycle, and the final extra loss was  
384 12.8%. For PlsCho, the additional loss compared to the control appeared slowly at the 7<sup>th</sup>  
385 cycle (11.9%,  $P < 0.05$  vs. freezing-only samples).

386 These findings are partially consistent with those of previous reports that lipid oxidation in  
387 meat products became worse after three or more cycles (Ali et al., 2015; Qingmin Chen et al.,  
388 2018). However, our results also indicated that for plasmalogens in fish meat, especially  
389 PlsEtn, this restriction should be reduced to only one cycle. Besides, because plasmalogens  
390 are fairly susceptible to quality deterioration, they might serve as a more sensitive tool for  
391 monitoring changes in the freshness of meat due to thawing.

392 Overall, our study revealed important behaviors in the loss of plasmalogens in ready-to-eat

393 raw fish during storage (including chilling, freezing, and thawing). One study limitation is  
394 that the determination of plasmalogen levels was based on a semi-quantitative profiling  
395 method by LC/MS, whereas it is desirable to perform absolute quantitation of total intact  
396 plasmalogens in future studies. Besides, only tuna meat was analyzed here, and the same  
397 investigation strategy could be extended to other food products containing plasmalogens at  
398 different concentrations and compositions. Since many disorders associated with metabolic  
399 syndrome (e.g., Alzheimer's disease) often have a long preclinical phase, diet could be more  
400 important in this phase than drugs for improving metabolic health. One associated strategy to  
401 this end is better preservation and control of functional components in foods, such as  
402 functional lipids represented by plasmalogens.

403

#### 404 **4. Conclusions**

405 This study explored the decrease of plasmalogens and the simultaneous global changes of  
406 related lipids in ready-to-eat raw tuna meat during storage, including chilling, freezing, and  
407 thawing. Long-term cold storage caused a considerable loss of plasmalogens, and the storage  
408 duration and temperature were important factors. In particular, chilling under 4 °C for 15  
409 days resulted in the loss of almost half of total plasmalogens. The plasmalogen fingerprints  
410 also showed characteristic changes during long-term storage. For the different headgroups,  
411 the ethanolamine type (i.e., PlsEtn) was less stable than the choline type (i.e., PlsCho). For  
412 the *sn*-2 fatty acyl chains, plasmalogen species containing PUFA were more likely to decrease

413 in concentration. In addition, although a single thawing step did not affect the plasmalogen  
414 level regardless of the employed thawing method, more than one freeze-thaw cycles led to  
415 extra loss of plasmalogens, especially PlsEtn. Regarding the possible mechanisms, the  
416 storage-induced plasmalogen loss might be attributed to oxidation and degradation. The  
417 accumulation of oxidized plasmalogens was strongly correlated with that of other lipid  
418 oxidation products and the degraded phospholipids, suggesting that plasmalogen loss could  
419 serve as a good indicator of meat quality deterioration. These findings not only provide  
420 additional information about the loss of functional phospholipids during food storage, but  
421 also indicate a more sensitive way to monitor the freshness and quality of ready-to-eat fish  
422 products.

423

#### 424 **Abbreviations**

425 Artificial neural network (ANN), collision-induced dissociation (CID), diglycerides (DG),  
426 electrospray ionization (ESI), extracted ion chromatogram (EIC), free fatty acids (FFA),  
427 liquid chromatography (LC), lysophosphatidylcholine (LPC), lysophosphatidylethanolamine  
428 (LPE), malonaldehyde (MDA), mass spectrometry (MS), phosphatidylcholine (PC),  
429 phosphatidylethanolamine (PE), polyunsaturated fatty acyls (PUFA), principal component  
430 analysis (PCA), standard deviation (SD), 1,1,3,3-tetraethoxypropane (TEP), thiobarbituric  
431 acid (TBA), thiobarbituric acid-reactive substances (TBARS), triglycerides (TG).

432

433 **Author contributions**

434 **Zhen Chen:** Conceptualization, Funding acquisition, Investigation, Methodology,  
435 Visualization, Writing - original draft. **Jiaping Jia:** Data curation, Formal analysis,  
436 Investigation, Methodology, Resources. **Yue Wu:** Data curation, Formal analysis,  
437 Methodology, Software, Validation, Visualization, Writing - original draft. **Hitoshi Chiba:**  
438 Resources, Validation, review & editing. **Shu-Ping Hui:** Resources, Project administration,  
439 Supervision.

440

441 **Conflict of interest**

442 The authors declare that they have no known competing financial interests or personal  
443 relationships that could have appeared to influence the work reported in this paper.

444

445 **Acknowledgments**

446 This work was supported by Japan Society for the Promotion of Science (JSPS) KAKENHI  
447 Grant No. 19K16531 and No. 21K14799.

448

449 **References**

- 450 Aguilera Barraza, F. A., León, R. A. Q., & Álvarez, P. X. L. (2015). Kinetics of protein and  
451 textural changes in Atlantic salmon under frozen storage. *Food Chemistry*, *182*, 120–  
452 127. <https://doi.org/10.1016/j.foodchem.2015.02.055>
- 453 Ali, S., Zhang, W., Rajput, N., Khan, M. A., Li, C. B., & Zhou, G. H. (2015). Effect of  
454 multiple freeze-thaw cycles on the quality of chicken breast meat. *Food Chemistry*, *173*,  
455 808–814. <https://doi.org/10.1016/j.foodchem.2014.09.095>
- 456 Ameer, K., Bae, S.-W., Jo, Y., Lee, H.-G., Ameer, A., & Kwon, J.-H. (2017). Optimization of  
457 microwave-assisted extraction of total extract, stevioside and rebaudioside-A from  
458 *Stevia rebaudiana* (Bertoni) leaves, using response surface methodology (RSM) and  
459 artificial neural network (ANN) modelling. *Food Chemistry*, *229*, 198–207.  
460 <https://doi.org/10.1016/j.foodchem.2017.01.121>
- 461 Aung, T., Kim, S.-J., & Eun, J.-B. (2022). A hybrid RSM-ANN-GA approach on optimisation  
462 of extraction conditions for bioactive component-rich laver (*Porphyra dentata*) extract.  
463 *Food Chemistry*, *366*, 130689. <https://doi.org/10.1016/j.foodchem.2021.130689>
- 464 Broniec, A., Klosinski, R., Pawlak, A., Wrona-Krol, M., Thompson, D., & Sarna, T. (2011).  
465 Interactions of plasmalogens and their diacyl analogs with singlet oxygen in selected  
466 model systems. *Free Radical Biology and Medicine*, *50*(7), 892–898.  
467 <https://doi.org/10.1016/j.freeradbiomed.2011.01.002>
- 468 Chen, Qingmin, Xie, Y., Xi, J., Guo, Y., Qian, H., Cheng, Y., Chen, Y., & Yao, W. (2018).  
469 Characterization of lipid oxidation process of beef during repeated freeze-thaw by  
470 electron spin resonance technology and Raman spectroscopy. *Food Chemistry*,  
471 *243*(September 2017), 58–64. <https://doi.org/10.1016/j.foodchem.2017.09.115>
- 472 Chen, Qinsheng, Wang, X., Cong, P., Liu, Y., Wang, Y., Xu, J., & Xue, C. (2017). Mechanism  
473 of Phospholipid Hydrolysis for Oyster *Crassostrea plicatula* Phospholipids During  
474 Storage Using Shotgun Lipidomics. *Lipids*, *52*(12), 1045–1058.  
475 <https://doi.org/10.1007/s11745-017-4305-7>
- 476 Chen, Z., Liang, Q., Wu, Y., Gao, Z., Kobayashi, S., Patel, J., Li, C., Cai, F., Zhang, Y., Liang,  
477 C., Chiba, H., & Hui, S.-P. (2020). Comprehensive lipidomic profiling in serum and  
478 multiple tissues from a mouse model of diabetes. *Metabolomics*, *16*(11), 115.  
479 <https://doi.org/10.1007/s11306-020-01732-9>
- 480 Coombs, C. E. O., Holman, B. W. B., Friend, M. A., & Hopkins, D. L. (2017). Long-term red  
481 meat preservation using chilled and frozen storage combinations: A review. *Meat*  
482 *Science*, *125*, 84–94. <https://doi.org/10.1016/j.meatsci.2016.11.025>
- 483 Ding, L., Zhang, L., Shi, H., Xue, C., Yanagita, T., Zhang, T., & Wang, Y. (2020). EPA-  
484 enriched ethanolamine plasmalogen alleviates atherosclerosis via mediating bile acids  
485 metabolism. *Journal of Functional Foods*, *66*(5), 103824.  
486 <https://doi.org/10.1016/j.jff.2020.103824>
- 487 Engelmann, B. (2004). Plasmalogens: targets for oxidants and major lipophilic antioxidants.

488 *Biochemical Society Transactions*, 32(1), 147–150. <https://doi.org/10.1042/bst0320147>

489 Folch, J., Lees, M., Stanley, G. H. S., & Sloane Stanley, G. H. (1957). A simple method for  
 490 the isolation and purification of total lipides from animal tissues. *The Journal of*  
 491 *Biological Chemistry*, 226(1), 497–509.

492 Guang, W., Tong, W., Wang, G., & Wang, T. (2010). The Role of Plasmalogen in the  
 493 Oxidative Stability of Neutral Lipids and Phospholipids. *Journal of Agricultural and*  
 494 *Food Chemistry*, 58(4), 2554–2561. <https://doi.org/10.1021/jf903906e>

495 Holzwarth, M., Korhummel, S., Carle, R., & Kammerer, D. R. (2012). Evaluation of the  
 496 effects of different freezing and thawing methods on color, polyphenol and ascorbic acid  
 497 retention in strawberries (*Fragaria×ananassa Duch.*). *Food Research International*,  
 498 48(1), 241–248. <https://doi.org/10.1016/j.foodres.2012.04.004>

499 Jang, J. E., Park, H. S., Yoo, H. J., Baek, I. J., Yoon, J. E., Ko, M. S., Kim, A. R., Kim, H. S.,  
 500 Park, H. S., Lee, S. E., Kim, S. W., Kim, S. J., Leem, J., Kang, Y. M., Jung, M. K., Pack,  
 501 C. G., Kim, C. J., Sung, C. O., Lee, I. K., ... Lee, K. U. (2017). Protective role of  
 502 endogenous plasmalogens against hepatic steatosis and steatohepatitis in mice.  
 503 *Hepatology*, 66(2), 416–431. <https://doi.org/10.1002/hep.29039>

504 Jiang, Q., Nakazawa, N., Hu, Y., Osako, K., & Okazaki, E. (2019). Changes in quality  
 505 properties and tissue histology of lightly salted tuna meat subjected to multiple freeze-  
 506 thaw cycles. *Food Chemistry*, 293(January), 178–186.  
 507 <https://doi.org/10.1016/j.foodchem.2019.04.091>

508 Karlsdottir, M. G., Sveinsdottir, K., Kristinsson, H. G., Villot, D., Craft, B. D., & Arason, S.  
 509 (2014). Effects of temperature during frozen storage on lipid deterioration of saithe  
 510 (*Pollachius virens*) and hoki (*Macruronus novaezelandiae*) muscles. *Food Chemistry*,  
 511 156, 234–242. <https://doi.org/10.1016/j.foodchem.2014.01.113>

512 Leygonie, C., Britz, T. J., & Hoffman, L. C. (2012). Impact of freezing and thawing on the  
 513 quality of meat: Review. *Meat Science*, 91(2), 93–98.  
 514 <https://doi.org/10.1016/j.meatsci.2012.01.013>

515 Li, D., Xie, H., Liu, Z., Li, A., Li, J., Liu, B., Liu, X., & Zhou, D. (2019). Shelf life prediction  
 516 and changes in lipid profiles of dried shrimp (*Penaeus vannamei*) during accelerated  
 517 storage. *Food Chemistry*, 297(February).  
 518 <https://doi.org/10.1016/j.foodchem.2019.124951>

519 Medina, S., Pereira, J. A., Silva, P., Perestrelo, R., & Câmara, J. S. (2019). Food fingerprints  
 520 – A valuable tool to monitor food authenticity and safety. *Food Chemistry*, 278, 144–  
 521 162. <https://doi.org/10.1016/j.foodchem.2018.11.046>

522 Morel, Y., Hegdekar, N., Sarkar, C., Lipinski, M. M., Kane, M. A., & Jones, J. W. (2021).  
 523 Structure-specific, accurate quantitation of plasmalogen glycerophosphoethanolamine.  
 524 *Analytica Chimica Acta*, 1186, 339088. <https://doi.org/10.1016/j.aca.2021.339088>

525 Pérez-Palacios, T., Ruiz, J., Dewettinck, K., Le, T. T., & Antequera, T. (2010). Muscle  
 526 individual phospholipid classes throughout the processing of dry-cured ham: Influence  
 527 of pre-cure freezing. *Meat Science*, 84(3), 431–436.

- 528 <https://doi.org/10.1016/j.meatsci.2009.09.012>
- 529 Prabhakar, P. K., Vatsa, S., Srivastav, P. P., & Pathak, S. S. (2020). A comprehensive review  
530 on freshness of fish and assessment: Analytical methods and recent innovations. *Food*  
531 *Research International*, 133(March), 109157.  
532 <https://doi.org/10.1016/j.foodres.2020.109157>
- 533 R Core Team. (2021). *R: A Language and Environment for Statistical Computing*.
- 534 Santos, J., Mendiola, J. A., Oliveira, M. B. P. P., Ibáñez, E., & Herrero, M. (2012). Sequential  
535 determination of fat- and water-soluble vitamins in green leafy vegetables during  
536 storage. *Journal of Chromatography A*, 1261, 179–188.  
537 <https://doi.org/10.1016/j.chroma.2012.04.067>
- 538 Sejimo, S., Hossain, M. S., & Akashi, K. (2018). Scallop-derived plasmalogens attenuate the  
539 activation of PKC $\delta$  associated with the brain inflammation. *Biochemical and*  
540 *Biophysical Research Communications*, 503(2), 837–842.  
541 <https://doi.org/10.1016/j.bbrc.2018.06.084>
- 542 Soyer, A., Özalp, B., Dalmiş, Ü., & Bilgin, V. (2010). Effects of freezing temperature and  
543 duration of frozen storage on lipid and protein oxidation in chicken meat. *Food*  
544 *Chemistry*, 120(4), 1025–1030. <https://doi.org/10.1016/j.foodchem.2009.11.042>
- 545 Stadelmann-Ingrand, S., Favreliere, S., Fauconneau, B., Mauco, G., & Tallineau, C. (2001).  
546 Plasmalogen degradation by oxidative stress: production and disappearance of specific  
547 fatty aldehydes and fatty  $\alpha$ -hydroxyaldehydes. *Free Radical Biology and Medicine*,  
548 31(10), 1263–1271. [https://doi.org/10.1016/S0891-5849\(01\)00720-1](https://doi.org/10.1016/S0891-5849(01)00720-1)
- 549 Su, X. Q., Wang, J., & Sinclair, A. J. (2019). Plasmalogens and Alzheimer's disease: A  
550 review. *Lipids in Health and Disease*, 18(1), 1–10. [https://doi.org/10.1186/s12944-019-](https://doi.org/10.1186/s12944-019-1044-1)  
551 [1044-1](https://doi.org/10.1186/s12944-019-1044-1)
- 552 Tappi, S., Pinheiro, A. C. D. A. S., Mercatante, D., Picone, G., Soglia, F., Rodriguez-Estrada,  
553 M. T., Petracci, M., Capozzi, F., & Rocculi, P. (2020). Quality changes during frozen  
554 storage of mechanical-separated flesh obtained from an underutilized crustacean. *Foods*,  
555 9(10). <https://doi.org/10.3390/foods9101485>
- 556 Wang, B., Kong, B., Li, F., Liu, Q., Zhang, H., & Xia, X. (2020). Changes in the thermal  
557 stability and structure of protein from porcine longissimus dorsi induced by different  
558 thawing methods. *Food Chemistry*, 316(August 2019).  
559 <https://doi.org/10.1016/j.foodchem.2020.126375>
- 560 Wang, J., Liao, J., Wang, H., Zhu, X., Li, L., Lu, W., Song, G., & Shen, Q. (2021).  
561 Quantitative and comparative study of plasmalogen molecular species in six edible  
562 shellfishes by hydrophilic interaction chromatography mass spectrometry. *Food*  
563 *Chemistry*, 334(January 2020), 127558. <https://doi.org/10.1016/j.foodchem.2020.127558>
- 564 Weisser, M., Vieth, M., Stolte, M., Riederer, P., Pfeuffer, R., Leblhuber, F., & Spiteller, G.  
565 (1997). Dramatic increase of  $\alpha$ -hydroxyaldehydes derived from plasmalogens in the  
566 aged human brain. *Chemistry and Physics of Lipids*, 90(1–2), 135–142.  
567 [https://doi.org/10.1016/S0009-3084\(97\)00089-3](https://doi.org/10.1016/S0009-3084(97)00089-3)

- 568 Wu, Y., Chen, Z., Chiba, H., & Hui, S.-P. (2020). Plasmalogen fingerprint alteration and  
569 content reduction in beef during boiling, roasting, and frying. *Food Chemistry*,  
570 322(April), 126764. <https://doi.org/10.1016/j.foodchem.2020.126764>
- 571 Wu, Y., Chen, Z., Darwish, W. S., Terada, K., Chiba, H., & Hui, S.-P. (2019). Choline and  
572 Ethanolamine Plasmalogens Prevent Lead-Induced Cytotoxicity and Lipid Oxidation in  
573 HepG2 Cells. *Journal of Agricultural and Food Chemistry*, 67(27), 7716–7725.  
574 <https://doi.org/10.1021/acs.jafc.9b02485>
- 575 Wu, Y., Chen, Z., Jia, J., Chiba, H., & Hui, S. (2021). Quantitative and Comparative  
576 Investigation of Plasmalogen Species in Daily Foodstuffs. *Foods*, 10(1), 124.  
577 <https://doi.org/10.3390/foods10010124>
- 578 Xia, X., Kong, B., Liu, J., Diao, X., & Liu, Q. (2012). Influence of different thawing methods  
579 on physicochemical changes and protein oxidation of porcine longissimus muscle. *LWT*  
580 - *Food Science and Technology*, 46(1), 280–286.  
581 <https://doi.org/10.1016/j.lwt.2011.09.018>
- 582 Xu, W., Xu, X., Zhou, G., Wang, D., & Li, C. (2008). Changes of intramuscular  
583 phospholipids and free fatty acids during the processing of Nanjing dry-cured duck.  
584 *Food Chemistry*, 110(2), 279–284. <https://doi.org/10.1016/j.foodchem.2007.11.044>
- 585 Yamashita, S., Kanno, S., Honjo, A., Otoki, Y., Nakagawa, K., Kinoshita, M., & Miyazawa,  
586 T. (2016). Analysis of Plasmalogen Species in Foodstuffs. *Lipids*, 51(2), 199–210.  
587 <https://doi.org/10.1007/s11745-015-4112-y>
- 588 Zhou, X., Zhou, D. Y., Liu, Z. Y., Yin, F. W., Liu, Z. Q., Li, D. Y., & Shahidi, F. (2019).  
589 Hydrolysis and oxidation of lipids in mussel *Mytilus edulis* during cold storage. *Food*  
590 *Chemistry*, 272(August 2018), 109–116. <https://doi.org/10.1016/j.foodchem.2018.08.019>
- 591

592 **Figure captions**

593 **Figure 1.** (A) Structure of plasmalogens consisting of a headgroup (ethanolamine or choline),  
594 a fatty chain linked by vinyl-ether bond at the *sn*-1 position, and a fatty acyl chain at the *sn*-2  
595 position. (B) Representative photographs of tuna lean meat samples on the 5<sup>th</sup> and 15<sup>th</sup> day of  
596 storage under 4 °C, -25 °C, -40 °C, and -80 °C. (C) Changes in the levels of total  
597 plasmalogens during long-term storage under 4 °C, -25 °C, -40 °C, and -80 °C.

598 **Figure 2.** (A) PCA score plots of plasmalogen profiles under different storage temperatures.  
599 From left to right: -80 °C, -40 °C, -25 °C, and 4 °C. (B) Comparison of PlsEtn, PlsCho, PE,  
600 and PC contents during long-term storage (up to 90 days under -25 °C, -40 °C, and -80 °C;  
601 and up to 15 days under 4 °C). (C) Changes in fatty acyl content in PlsEtn and PlsCho during  
602 long-term storage (up to 90 days under -25 °C, -40 °C, and -80 °C; and up to 15 days under  
603 4 °C).

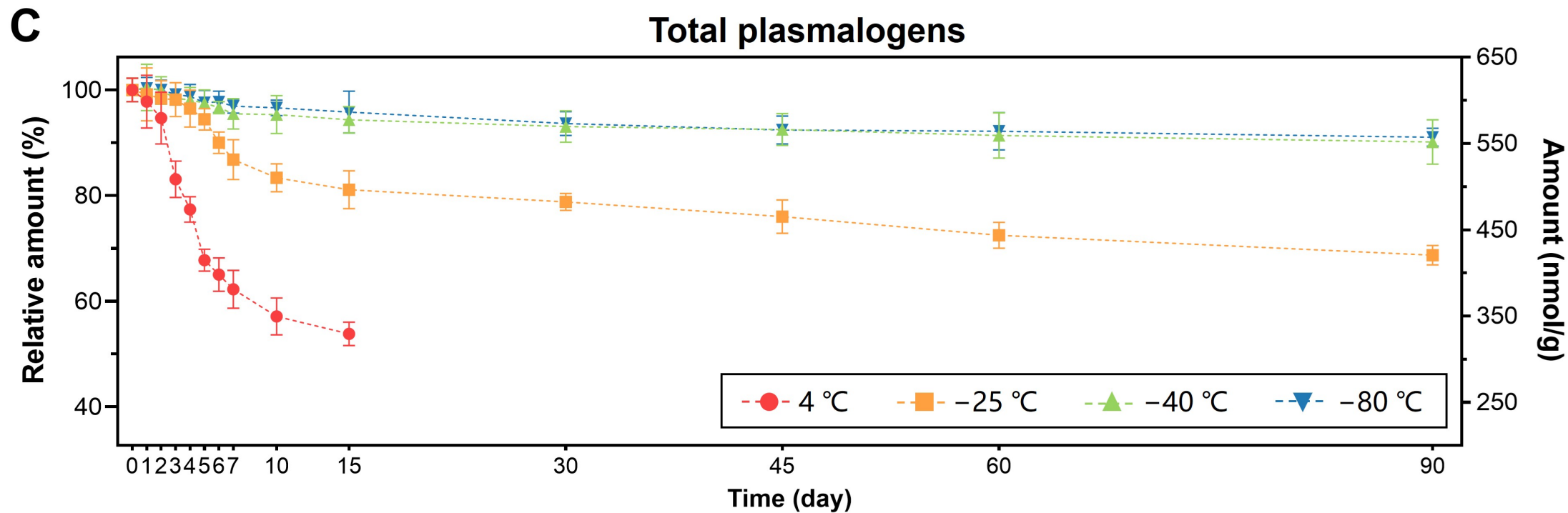
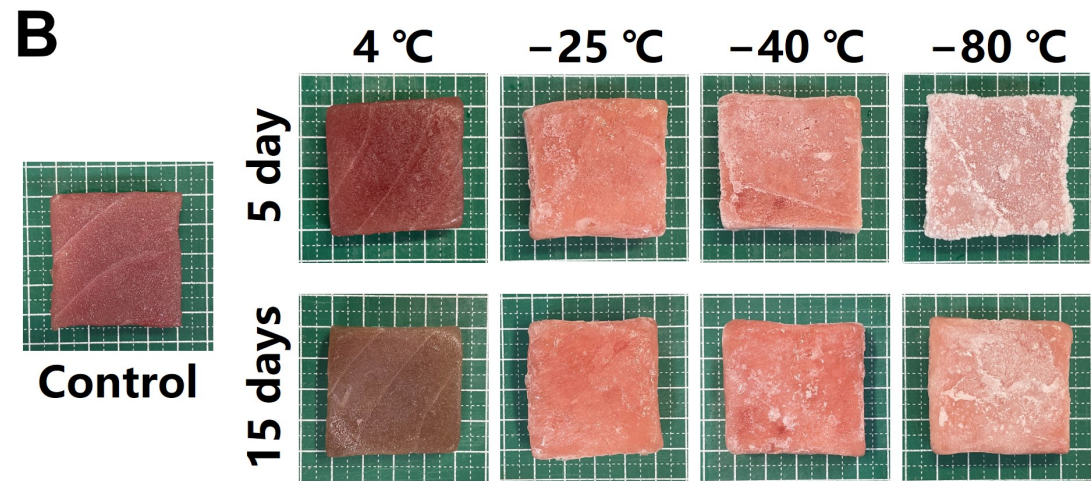
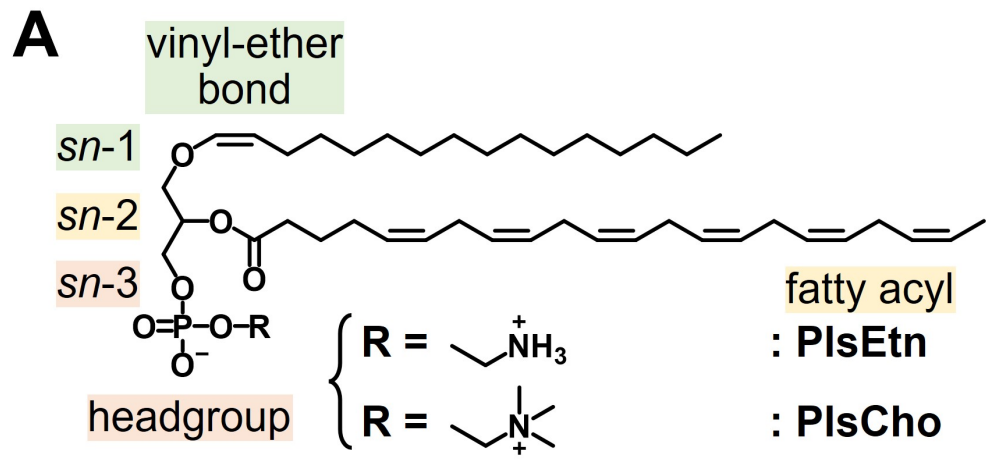
604 **Figure 3.** (A) Identification of oxidized plasmalogens by HR-MS and tandem MS, taking  
605 PlsEtn 38:6+4[O] as an example. HR-MS provided the chemical formula of  $C_{43}H_{74}O_{11}NP^-$ ,  
606 indicating the existence of PlsEtn 38:6 + 4[O]. Further MS<sup>2</sup> and MS<sup>3</sup> analyses confirmed the  
607 mixture of isomers PlsEtn p16:0(epo)/22:6(OH)(OOH) and PlsEtn p16:0(OH)<sub>2</sub>(OOH). (B)  
608 Accumulation of the oxidized PlsEtn and oxidized PlsCho (calculated as the sum of all  
609 species) during storage under 4 °C, -25 °C, and -40 °C.

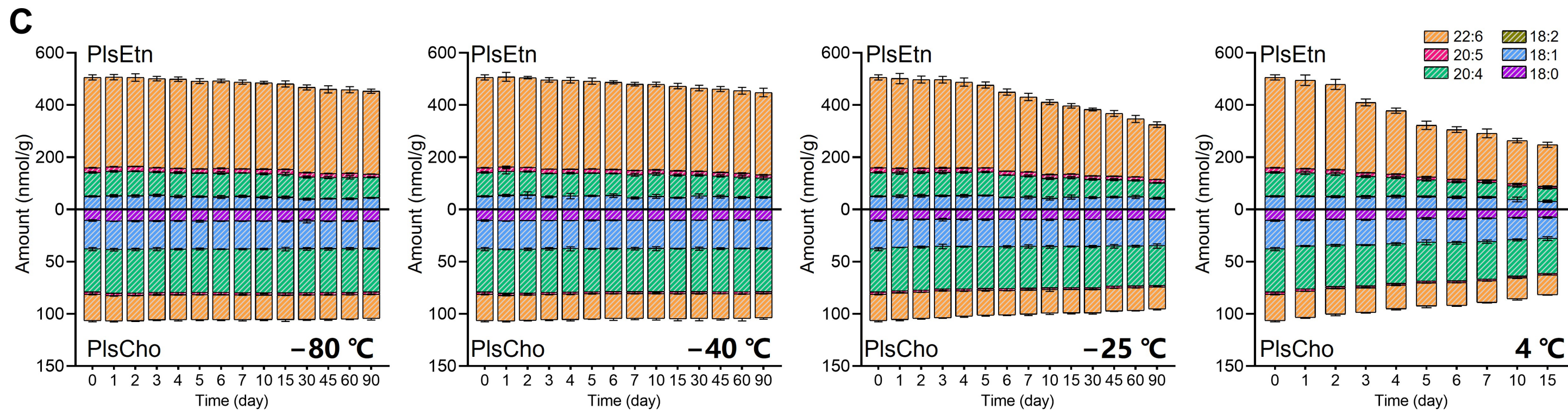
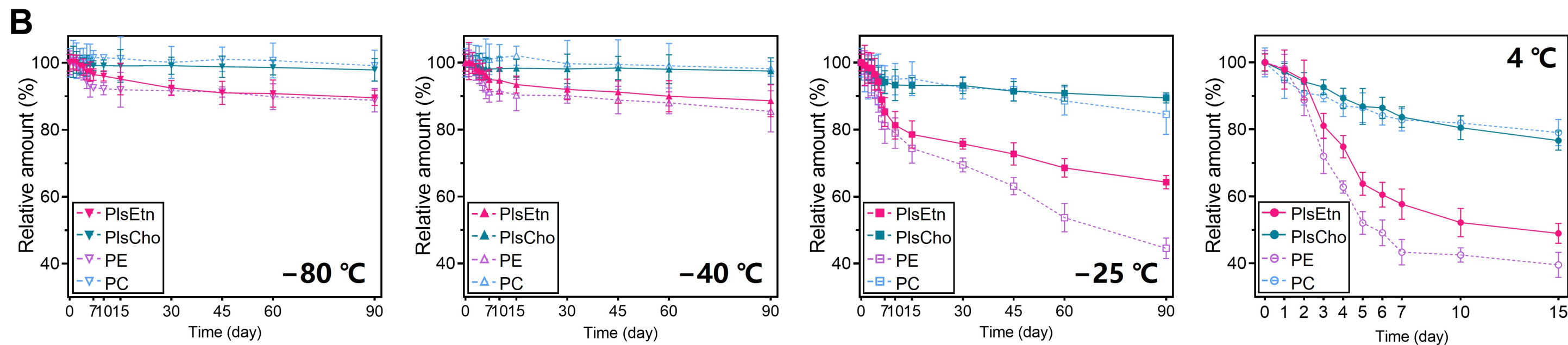
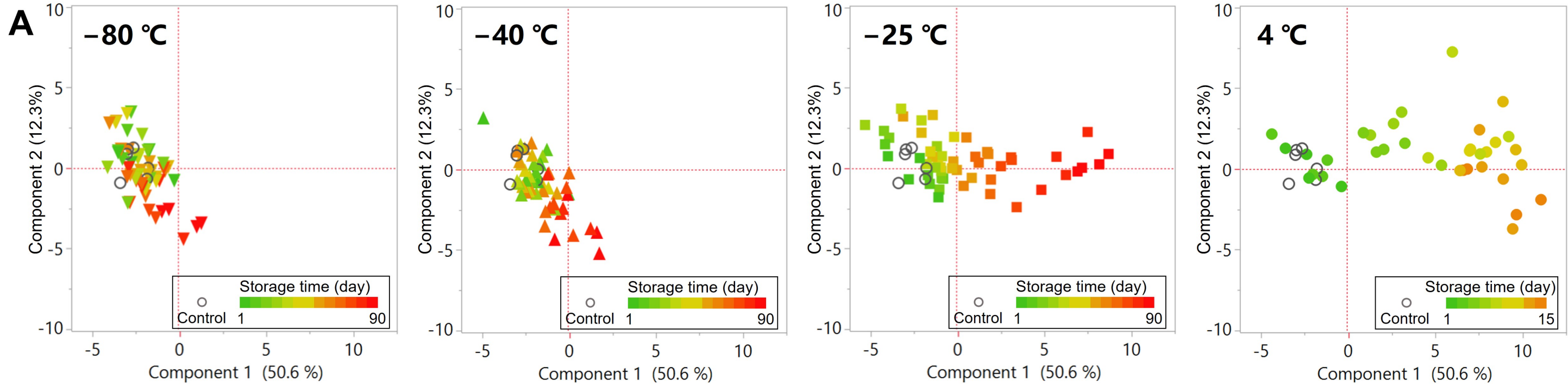
610 **Figure 4.** (A) Accumulation of lipid oxidation products (TG, DG, FFA, PC, and PE) during  
611 storage under 4 °C, -25 °C, and -40 °C. (B) TBARS levels during storage under 4 °C,

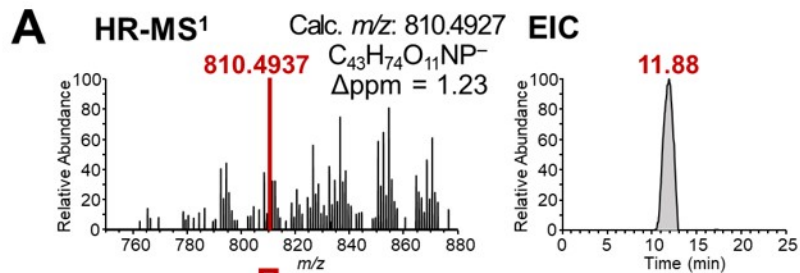
612 -25 °C, -40 °C, and -80 °C. (C) Increase in the levels of degraded phospholipids, namely  
613 LPC, LPE, and FFA during storage under 4 °C, -25 °C, -40 °C, and -80 °C.

614 **Figure 5.** (A) Heatmap of the Spearman's correlation coefficients between the loss of  
615 plasmalogens and the increase in the levels of related oxidized and degraded lipids. (B)  
616 Scatter plots of TBARS level versus the loss rate of total plasmalogens under 4 °C, -25 °C,  
617 -40 °C, and -80 °C. (C) Predictive three-dimensional surface plots of the remaining total  
618 plasmalogens, PlsEtn, and PlsCho during long-term storage under different temperatures.

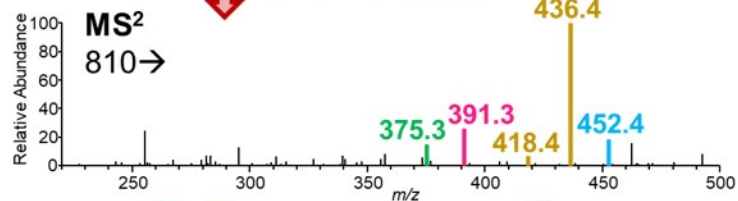
619 **Figure 6.** (A) Comparison of the contents of total plasmalogens, PlsEtn, and PlsCho in frozen  
620 samples thawed using different methods. Con = control, WT = water immersion thawing,  
621 MT = microwave thawing, RT = refrigerator thawing, AT = air thawing. (B) Comparison of  
622 the contents of total plasmalogens, PlsEtn, and PlsCho during multiple freeze-thaw cycles. \*,  
623  $P < 0.05$ , \*\*,  $P < 0.01$ , \*\*\*,  $P < 0.001$ , calculated using one-way ANOVA (using Tukey's  
624 post hoc test).







PlsEtn 38:6+4[O]

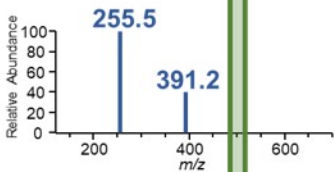


sn-1:  
p16:0+ [O]

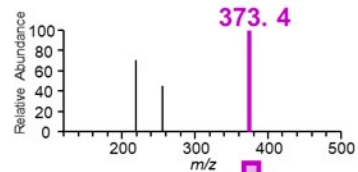
sn-2:  
22:6+3 [O]

sn-1: p16:0  
sn-2: 22:6+4 [O]

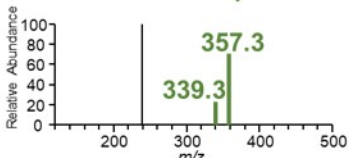
**MS<sup>3</sup>**  
810 → 452 →



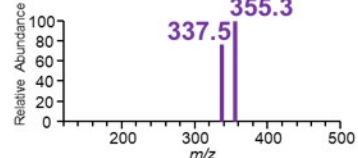
**MS<sup>3</sup>**  
810 → 391 →



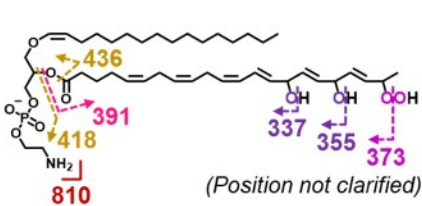
**MS<sup>3</sup>**  
810 → 375 →



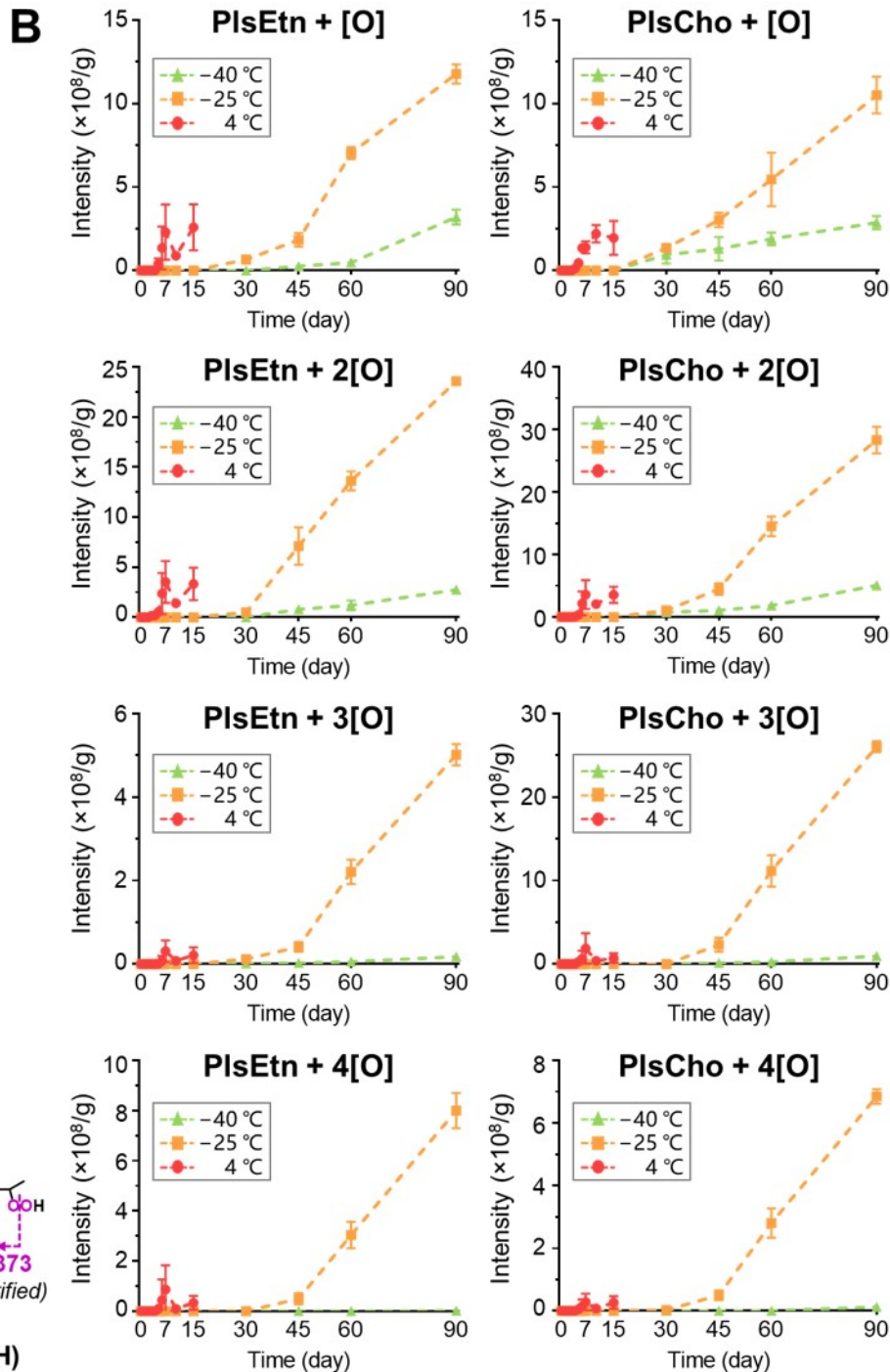
**MS<sup>4</sup>**  
810 → 391 → 373

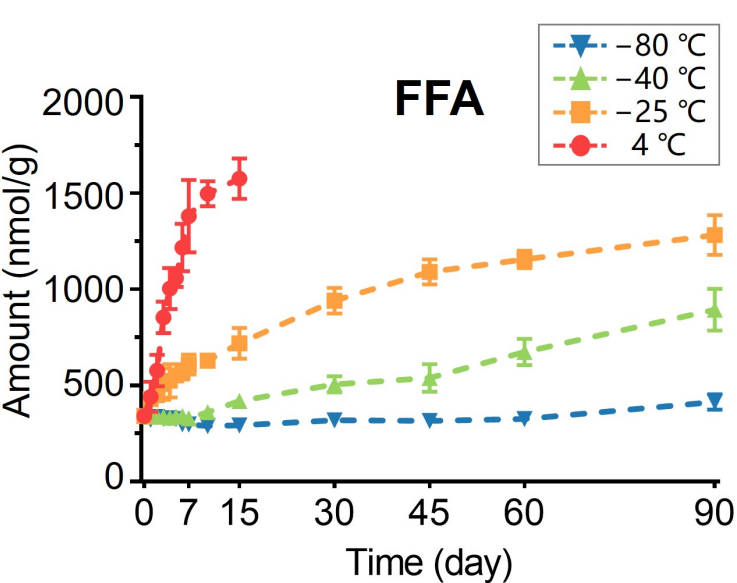
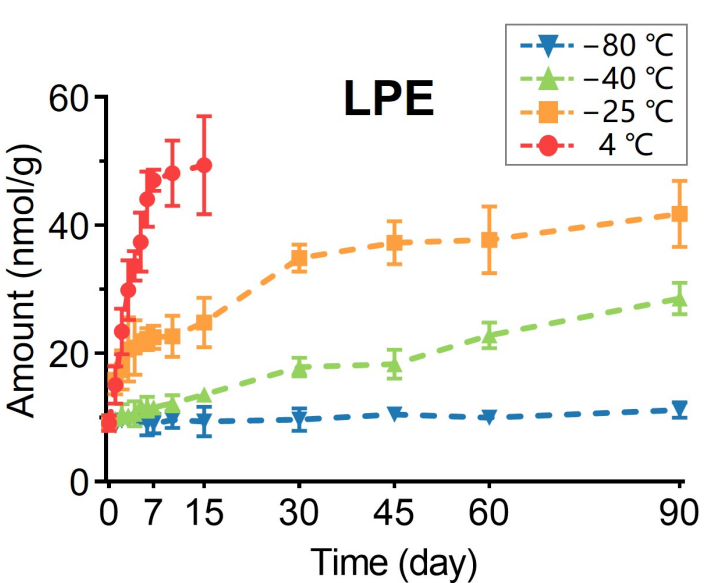
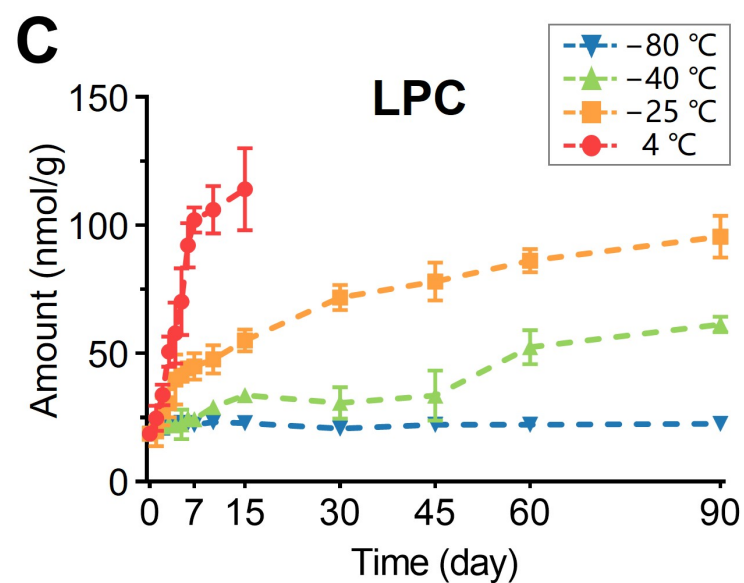
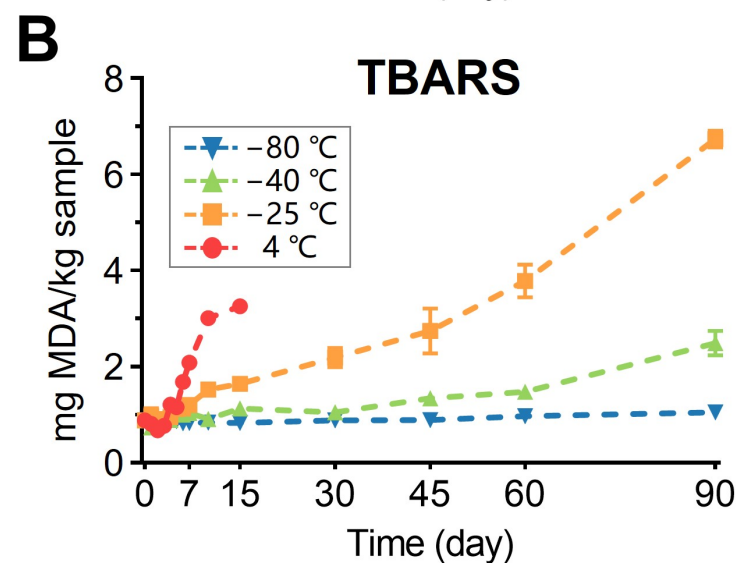
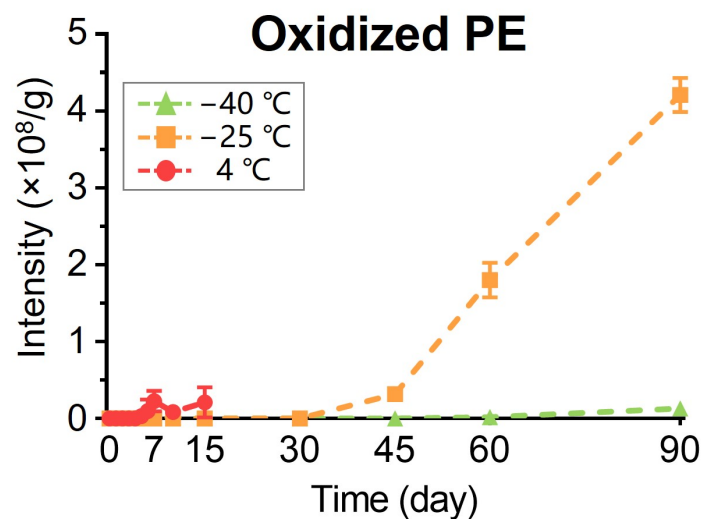
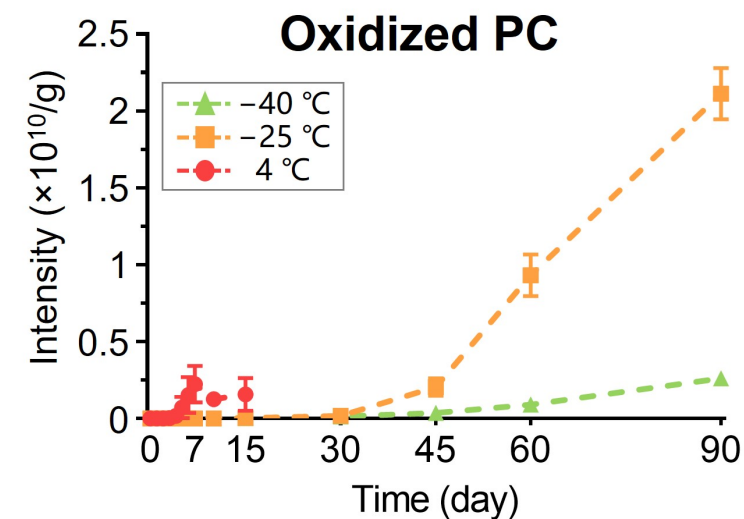
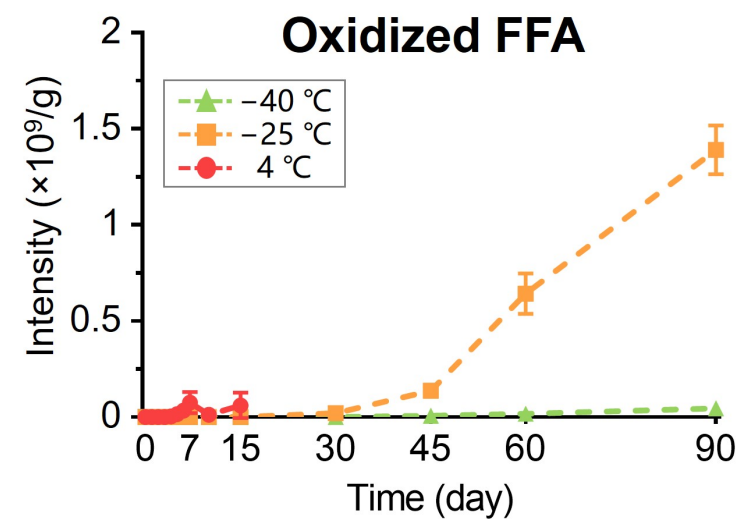
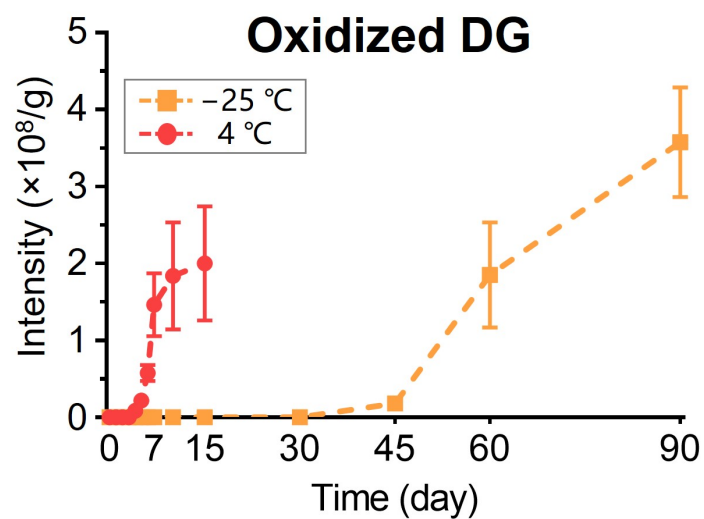
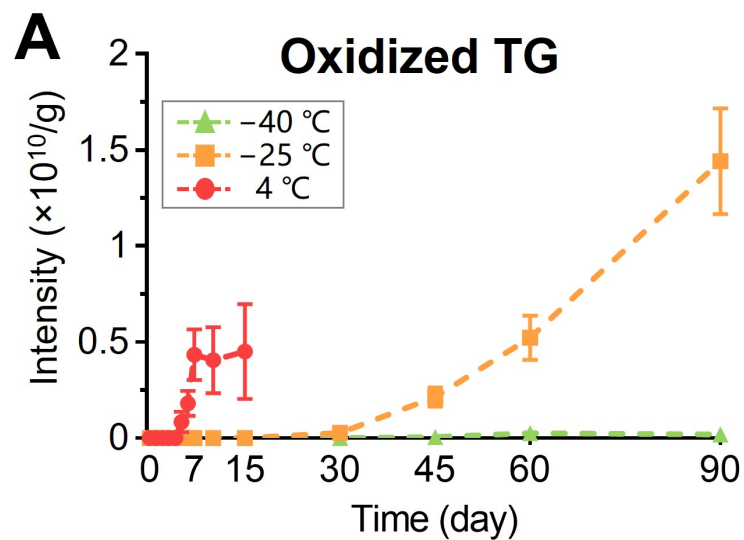


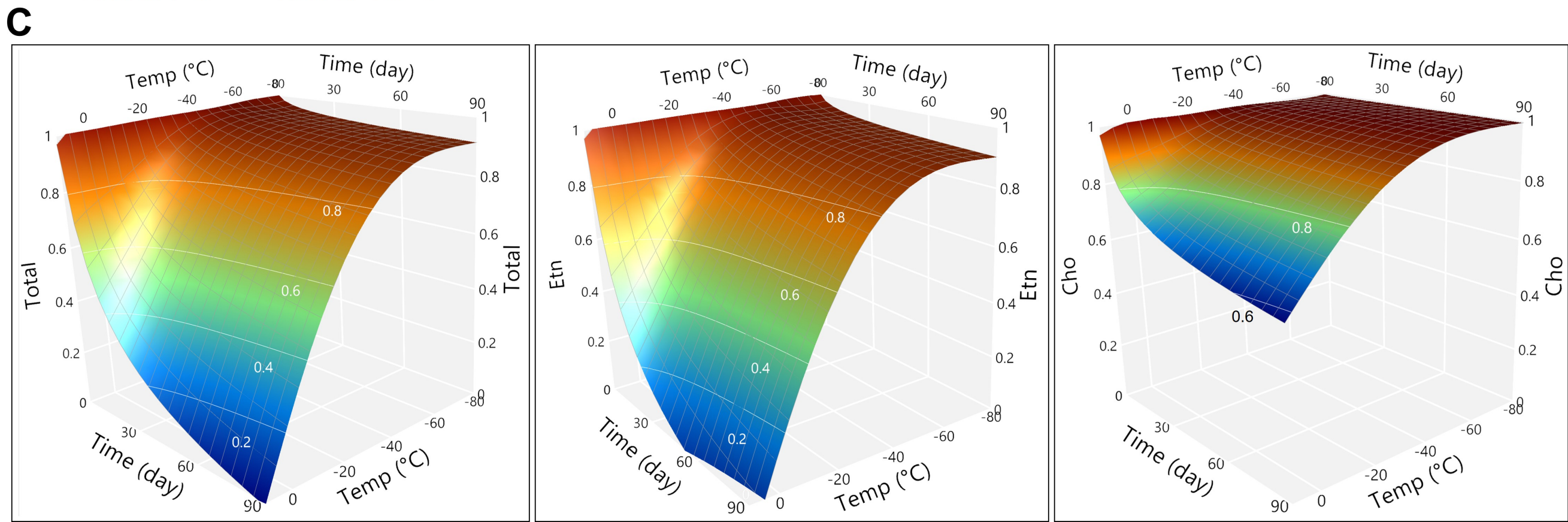
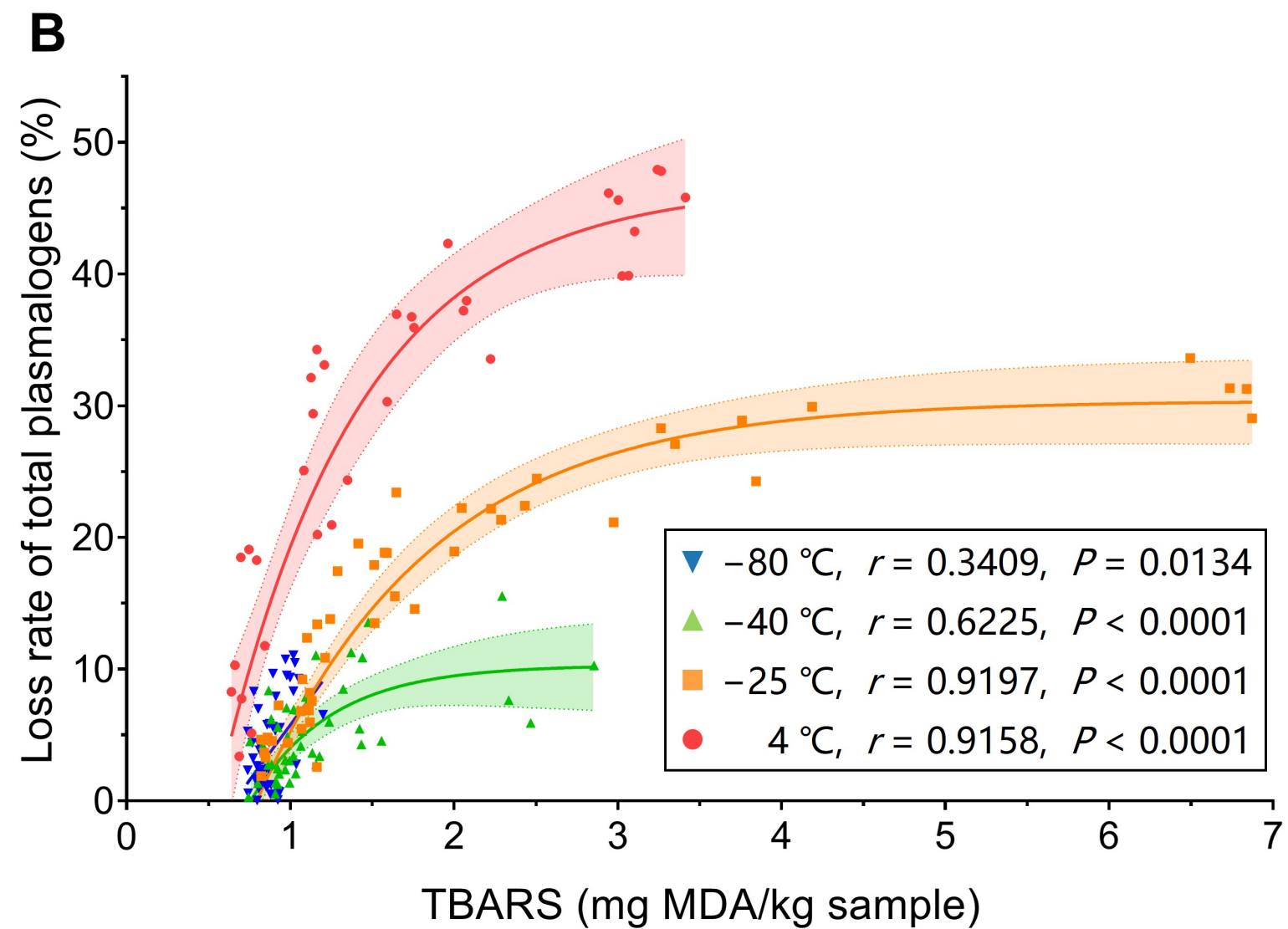
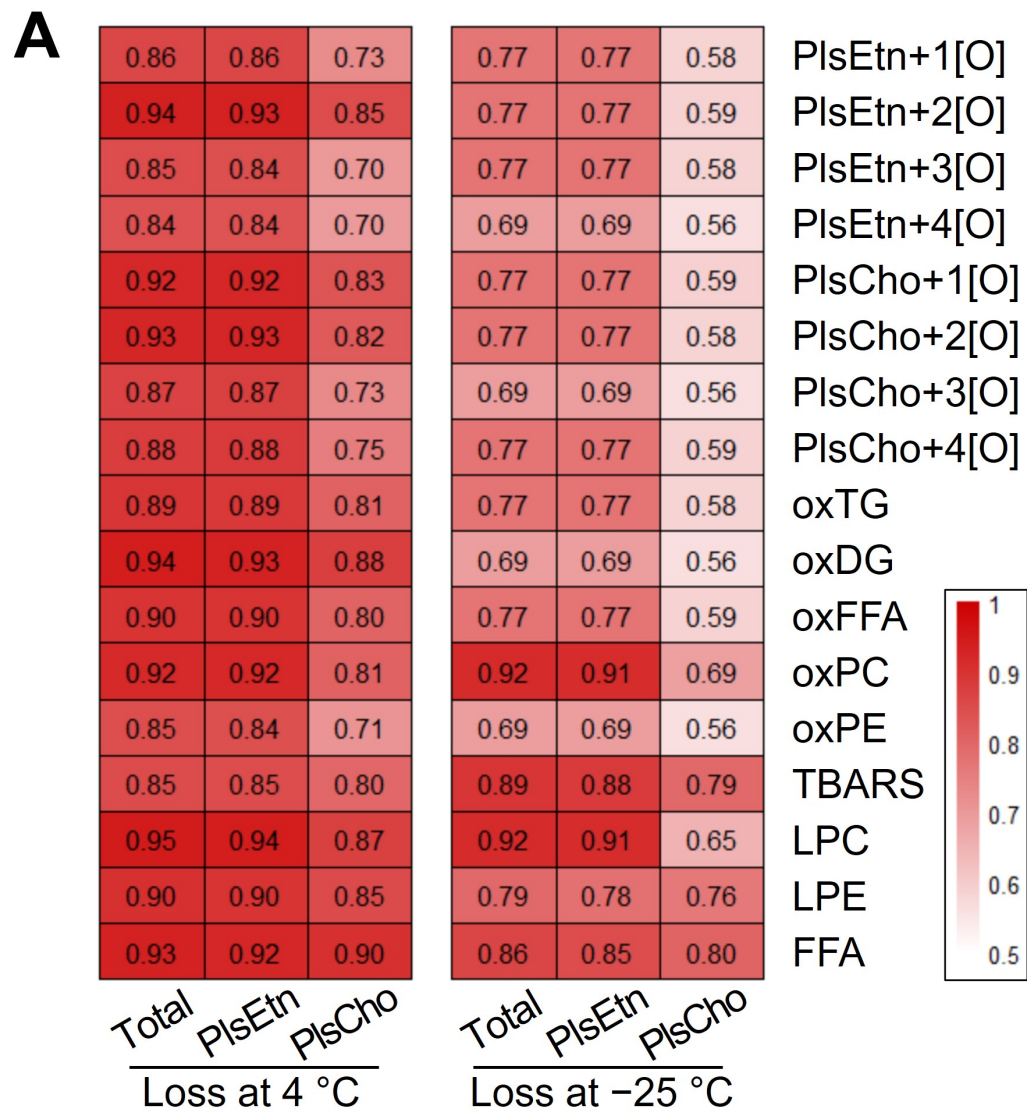
PlsEtn p16:0(epo)/22:6(OH)(OOH)

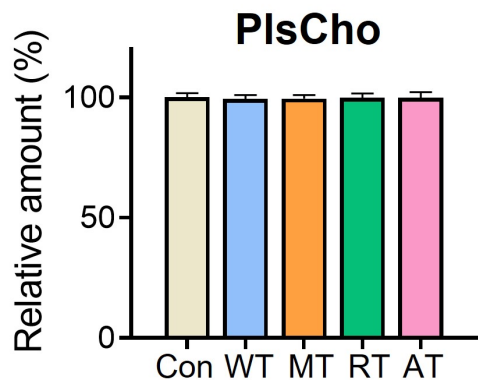
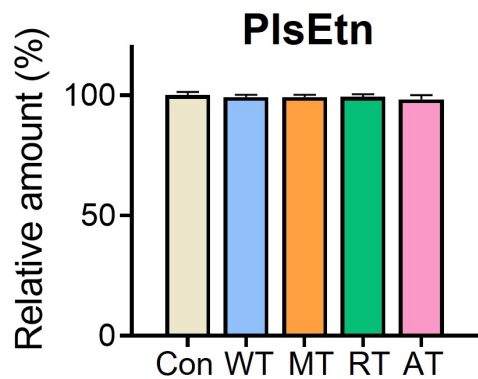
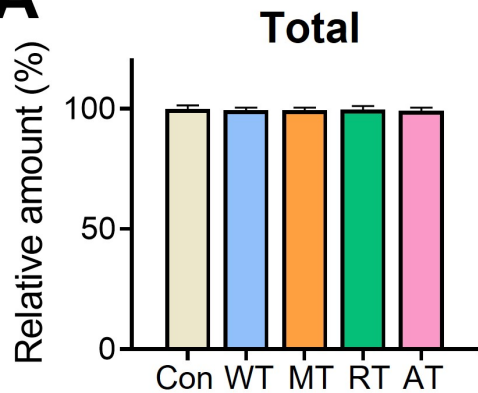
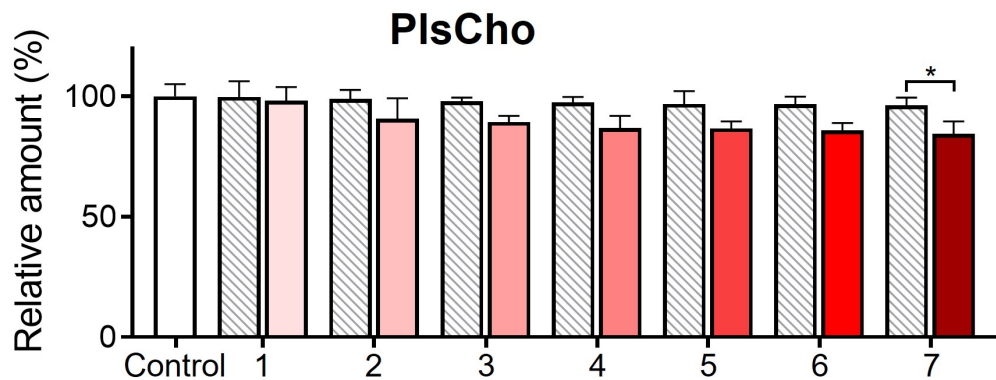
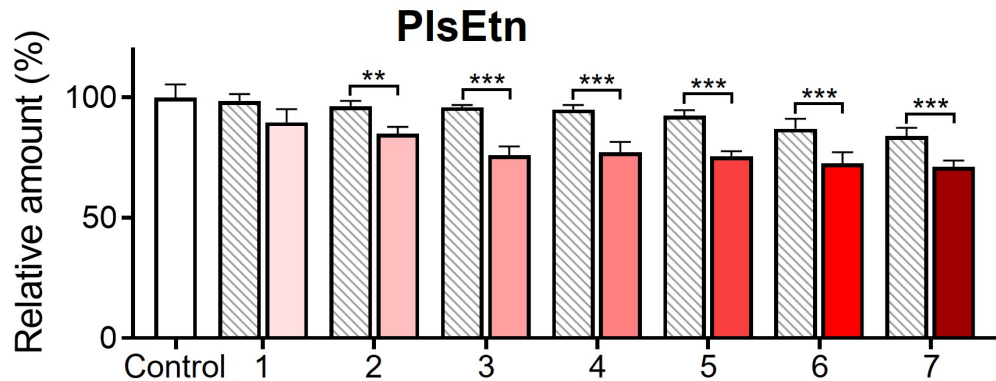
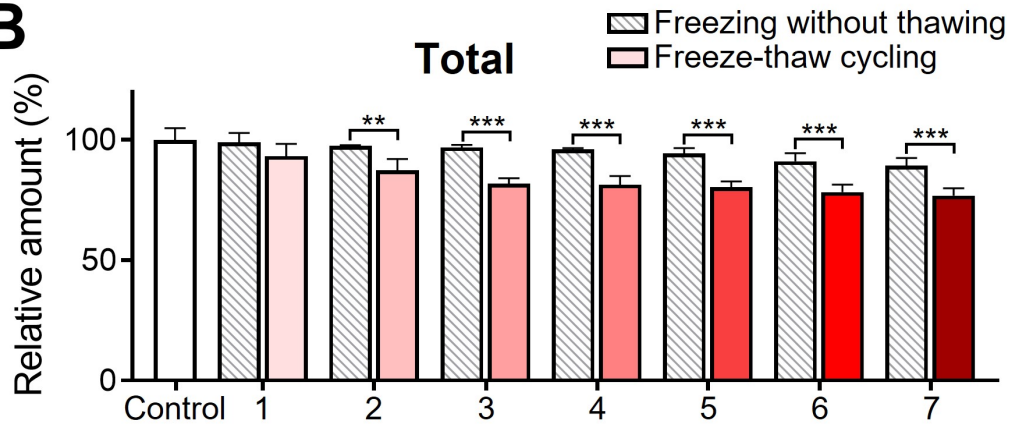


PlsEtn p16:0/22:6(OH)<sub>2</sub>(OOH)







**A****B**

## Supplementary

Table S1. Information of each lipid internal standard

Standard	Source	Concentration in MeOH stock solution (nmol/mL)	Amount in each sample (nmol/per tube)
Choline plasmalogen p16:0/17:0 (PlsCho p16:0/17:0)	Laboratory	15.0	1.5
Ethanolamine plasmalogen p16:0/17:0 (PlsEtn p16:0/17:0)	Laboratory	10.0	1.0
Phosphatidylcholine (PC 13:0/13:0)	Avanti Polar Lipids	15.0	1.5
Phosphatidylethanolamine (PE 15:0/15:0)	Avanti Polar Lipids	10.0	1.0
Lysophosphatidylcholine (LPC 15:0)	Avanti Polar Lipids	15.0	1.5
Lysophosphatidylethanolamine (LPE 13:0)	Avanti Polar Lipids	10.0	1.0
Free fatty acid (FFA 17:0)	Sigma-Aldrich	10.0	1.0

Table S2. Identification of intact plasmalogens in fish samples

Lipid species	Retention time (min)	Ion	Calc. <i>m/z</i>	Exp. <i>m/z</i>	$\Delta$ ppm	MS/MS signals	Molecule species
<b>PlsEtn</b>							
PlsEtn32:1	15.48	[M-H] <sup>-</sup>	672.4974	672.4987	-1.93	281,408,390	p14:0/18:1
						253,436,418	p16:0/16:1
PlsEtn34:1	16.39	[M-H] <sup>-</sup>	700.5287	700.5287	0.00	281,436,418	p16:0/18:1
PlsEtn34:2	15.85	[M-H] <sup>-</sup>	698.5130	698.5127	0.43	279,436,418	p16:0/18:2
						281,434,416	p16:1/18:1
PlsEtn34:4	14.92	[M-H] <sup>-</sup>	694.4817	694.4829	-1.73	303,408,390	p14:0/20:4
PlsEtn34:5	14.47	[M-H] <sup>-</sup>	692.4661	692.4673	-1.73	301,408,390	p14:0/20:5
PlsEtn36:1	17.17	[M-H] <sup>-</sup>	728.5600	728.5584	2.20	281,464,446	p18:0/18:1
PlsEtn36:2	16.51	[M-H] <sup>-</sup>	726.5443	726.5448	-0.69	281,462,444	p18:1/18:1
PlsEtn36:4	15.73	[M-H] <sup>-</sup>	722.5130	722.5150	-2.77	303,436,418	p16:0/20:4
PlsEtn36:5	15.29	[M-H] <sup>-</sup>	720.4974	720.4991	-2.36	301,436,418	p16:0/20:5
PlsEtn36:6	14.80	[M-H] <sup>-</sup>	718.4817	718.4825	-1.11	327,408,390	p14:0/22:6
PlsEtn38:4	16.58	[M-H] <sup>-</sup>	750.5443	750.5442	0.13	303,464,446	p18:0/20:4
						303,462,444	p18:1/20:4
PlsEtn38:5	16.07	[M-H] <sup>-</sup>	748.5287	748.5301	-1.87	329,436,418	p16:0/22:5
						301,464,446	p18:0/20:5
						327,436,418	p16:0/22:6
PlsEtn38:6	15.66	[M-H] <sup>-</sup>	746.5130	746.5146	-2.14	301,460,442	p18:2/20:5
PlsEtn38:7	14.95	[M-H] <sup>-</sup>	744.4974	744.4989	-2.01	327,434,416	p16:1/22:6
						301,460,442	p18:2/20:5
PlsEtn38:8	14.43	[M-H] <sup>-</sup>	742.4817	742.4819	-0.27	327,432,414	p16:2/22:6
PlsEtn40:6	16.45	[M-H] <sup>-</sup>	774.5443	774.5457	-1.81	327,464,446	p18:0/22:6
PlsEtn40:7	15.79	[M-H] <sup>-</sup>	772.5287	772.5292	-0.65	327,462,444	p18:1/22:6
PlsEtn40:8	15.29	[M-H] <sup>-</sup>	770.5130	770.5132	-0.26	327,460,442	p18:2/22:6
<b>PlsCho</b>							
PlsCho34:0	18.70	[M+CH <sub>3</sub> COO] <sup>-</sup>	804.6124	804.6125	-0.12	730,283,464	p16:0/18:0
PlsCho34:1	17.97	[M+CH <sub>3</sub> COO] <sup>-</sup>	802.5967	802.5984	-2.12	728,281,464	p16:0/18:1
PlsCho36:4	16.10	[M+CH <sub>3</sub> COO] <sup>-</sup>	824.5811	824.5811	0.00	750,303,464	p16:0/20:4
PlsCho36:5	15.10	[M+CH <sub>3</sub> COO] <sup>-</sup>	822.5654	822.5668	-1.70	748,301,464	p16:0/20:5
PlsCho38:4	17.76	[M+CH <sub>3</sub> COO] <sup>-</sup>	852.6124	852.6118	0.70	778,303,492	p18:0/20:4
PlsCho38:5	16.26	[M+CH <sub>3</sub> COO] <sup>-</sup>	850.5967	850.5972	-0.59	776,303,490	p18:1/20:4
PlsCho38:6	15.82	[M+CH <sub>3</sub> COO] <sup>-</sup>	848.5811	848.5824	-1.53	774,327,464	p16:0/22:6
PlsCho40:6	17.62	[M+CH <sub>3</sub> COO] <sup>-</sup>	876.6124	876.6124	0.00	802,327,492	p18:0/22:6

Table S3. Identification of oxidized plasmalogens in fish samples

Lipid species	Retention time (min)	Ion	Calc. <i>m/z</i>	Exp <i>m/z</i>	$\Delta$ ppm
<b>PlsEtn+1[O]</b>					
PlsEtn36:4+1[O]	14.13	[M-H] <sup>-</sup>	738.5079	738.5084	-0.68
PlsEtn38:4+1[O]	14.91	[M-H] <sup>-</sup>	766.5392	766.5388	0.52
PlsEtn38:5+1[O]	14.49	[M-H] <sup>-</sup>	764.5236	764.5250	-1.83
PlsEtn38:6+1[O]	13.95	[M-H] <sup>-</sup>	762.5079	762.5082	-0.39
PlsEtn40:6+1[O]	14.67	[M-H] <sup>-</sup>	790.5392	790.5394	-0.25
PlsEtn40:7+1[O]	14.10	[M-H] <sup>-</sup>	788.5236	788.5234	0.25
PlsEtn40:8+1[O]	14.04	[M-H] <sup>-</sup>	786.5079	786.5079	0.00
<b>PlsCho+1[O]</b>					
PlsCho38:5+1[O]	14.97	[M+CH <sub>3</sub> COO] <sup>-</sup>	866.5917	866.5913	0.46
PlsCho38:6+1[O]	14.22	[M+CH <sub>3</sub> COO] <sup>-</sup>	864.5760	864.5763	-0.35
<b>PlsEtn+2[O]</b>					
PlsEtn36:4+2[O]	13.83	[M-H] <sup>-</sup>	754.5028	754.5023	0.66
PlsEtn38:4+2[O]	14.46	[M-H] <sup>-</sup>	782.5341	782.5346	-0.64
PlsEtn38:5+2[O]	13.95	[M-H] <sup>-</sup>	780.5185	780.5181	0.51
PlsEtn38:6+2[O]	13.56	[M-H] <sup>-</sup>	778.5028	778.5028	0.00
PlsEtn40:6+2[O]	14.58	[M-H] <sup>-</sup>	806.5341	806.5345	-0.50
PlsEtn40:7+2[O]	13.62	[M-H] <sup>-</sup>	804.5185	804.5189	-0.50
<b>PlsCho+2[O]</b>					
PlsCho36:4+2[O]	14.25	[M+CH <sub>3</sub> COO] <sup>-</sup>	856.5709	856.5715	-0.70
PlsCho36:5+2[O]	13.43	[M+CH <sub>3</sub> COO] <sup>-</sup>	854.5553	854.5532	2.46
PlsCho38:5+2[O]	14.25	[M+CH <sub>3</sub> COO] <sup>-</sup>	882.5866	882.5860	0.68
PlsCho38:6+2[O]	13.77	[M+CH <sub>3</sub> COO] <sup>-</sup>	880.5709	880.5718	-1.02
PlsCho40:6+2[O]	15.64	[M+CH <sub>3</sub> COO] <sup>-</sup>	908.6022	908.6025	-0.33
<b>PlsEtn+3[O]</b>					
PlsEtn38:4+3[O]	13.26	[M-H] <sup>-</sup>	798.5291	798.5295	-0.50
PlsEtn38:5+3[O]	12.41	[M-H] <sup>-</sup>	796.5134	796.5143	-1.13
PlsEtn38:6+3[O]	12.21	[M-H] <sup>-</sup>	794.4978	794.4985	-0.88
PlsEtn38:7+3[O]	12.08	[M-H] <sup>-</sup>	792.4821	792.4830	-1.14
PlsEtn40:6+3[O]	12.68	[M-H] <sup>-</sup>	822.5291	822.5297	-0.73
PlsEtn40:7+3[O]	12.35	[M-H] <sup>-</sup>	820.5134	820.5151	-2.07
PlsEtn40:8+3[O]	12.24	[M-H] <sup>-</sup>	818.4978	818.4980	-0.24

Lipid species	Retention time (min)	Ion	Calc. <i>m/z</i>	Exp <i>m/z</i>	$\Delta$ ppm
<b>PlsCho+3[O]</b>					
PlsCho36:4+3[O]	13.59	[M+CH <sub>3</sub> COO] <sup>-</sup>	872.5658	872.5653	0.57
PlsCho36:5+3[O]	13.20	[M+CH <sub>3</sub> COO] <sup>-</sup>	870.5502	870.5505	-0.34
PlsCho38:5+3[O]	14.13	[M+CH <sub>3</sub> COO] <sup>-</sup>	898.5815	898.5814	0.11
PlsCho38:6+3[O]	13.46	[M+CH <sub>3</sub> COO] <sup>-</sup>	896.5658	896.5662	-0.45
PlsCho40:6+3[O]	14.55	[M+CH <sub>3</sub> COO] <sup>-</sup>	924.5971	924.5977	-0.65
<b>PlsEtn+4[O]</b>					
PlsEtn36:4+4[O]	12.02	[M-H] <sup>-</sup>	786.4927	786.4907	2.54
PlsEtn38:5+4[O]	12.02	[M-H] <sup>-</sup>	812.5083	812.5085	-0.25
PlsEtn38:6+4[O]	11.88	[M-H] <sup>-</sup>	810.4927	810.4937	-1.23
PlsEtn38:7+4[O]	11.64	[M-H] <sup>-</sup>	808.4770	808.4782	-1.48
PlsEtn40:6+4[O]	12.18	[M-H] <sup>-</sup>	838.5240	838.5257	-2.03
<b>PlsCho+4[O]</b>					
PlsCho38:5+4[O]	13.32	[M+CH <sub>3</sub> COO] <sup>-</sup>	914.5764	914.5787	-2.51
PlsCho38:6+4[O]	12.71	[M+CH <sub>3</sub> COO] <sup>-</sup>	912.5608	912.5616	-0.88
PlsCho40:6+4[O]	13.59	[M+CH <sub>3</sub> COO] <sup>-</sup>	940.5921	940.5923	-0.21

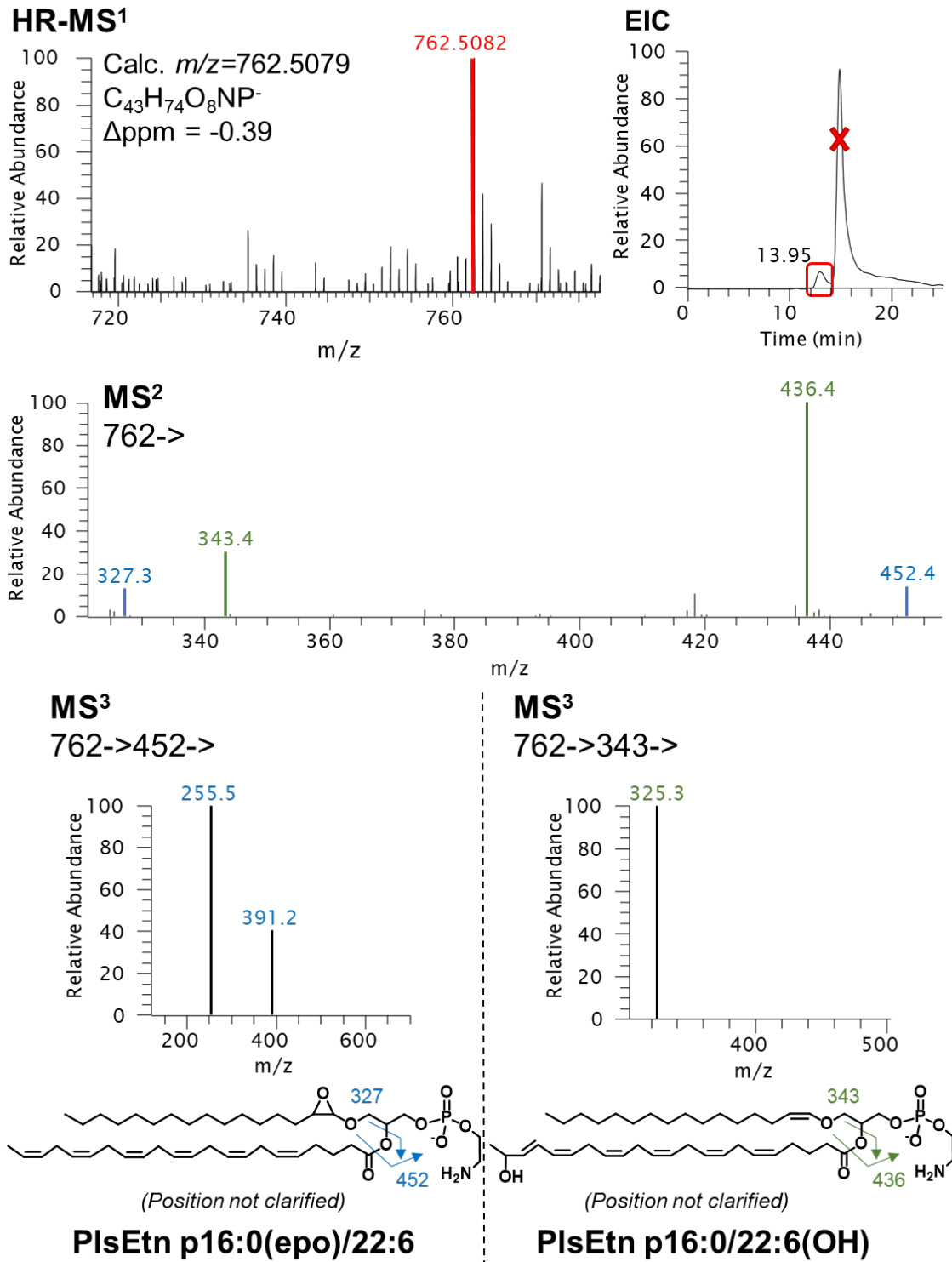


Figure S1. Identification of PlsEtn 38:6+1[O] by HR-MS and tandem MS.

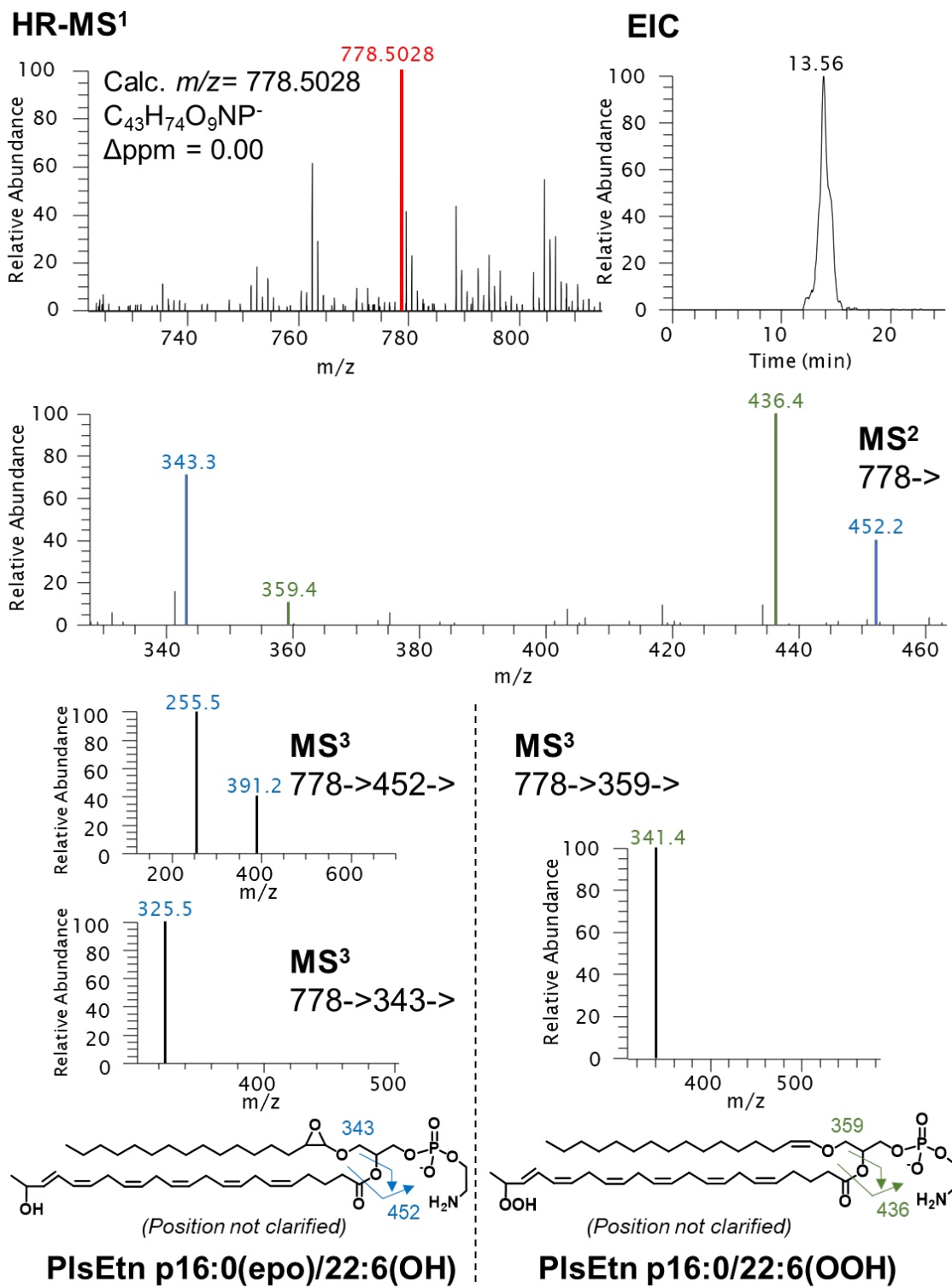
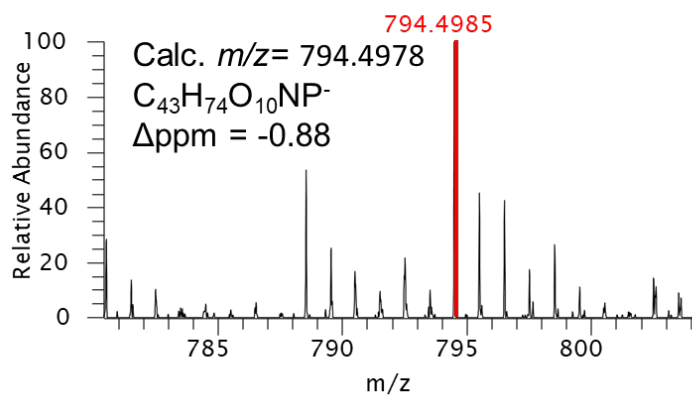
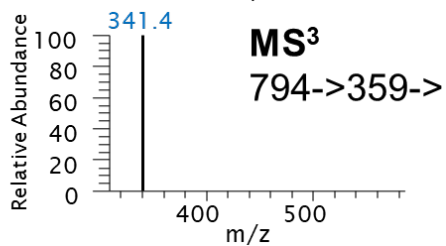
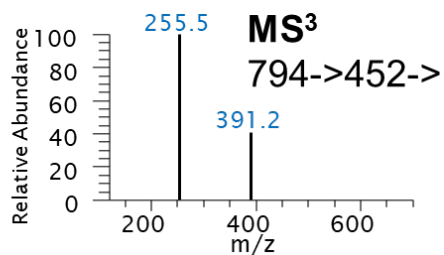
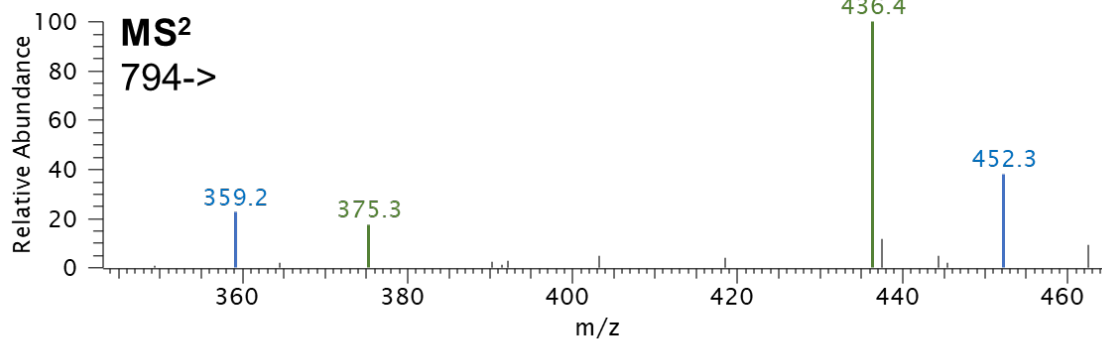
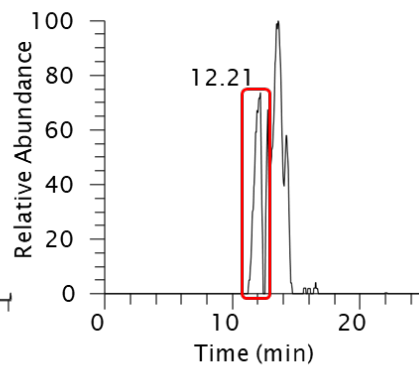


Figure S2. Identification of PlsEtn 38:6+2[O] by HR-MS and tandem MS.

### HR-MS<sup>1</sup>

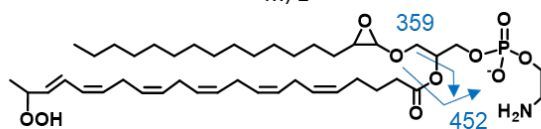
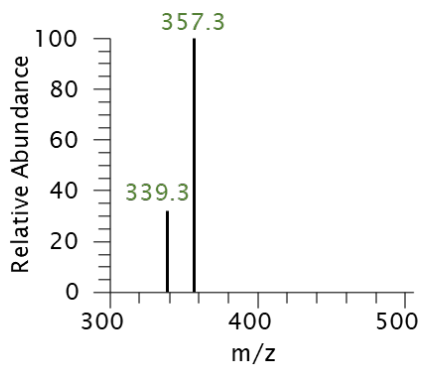


### EIC

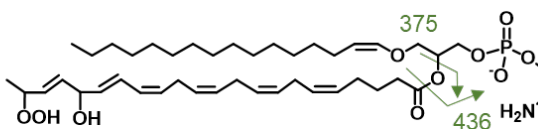


### MS<sup>3</sup>

794->375->



**PlsEtn p16:0(epo)/22:6(OOH)**



**PlsEtn p16:0/22:6(OH)(OOH)**

Figure S3. Identification of PlsEtn 38:6+3[O] by HR-MS and tandem MS.

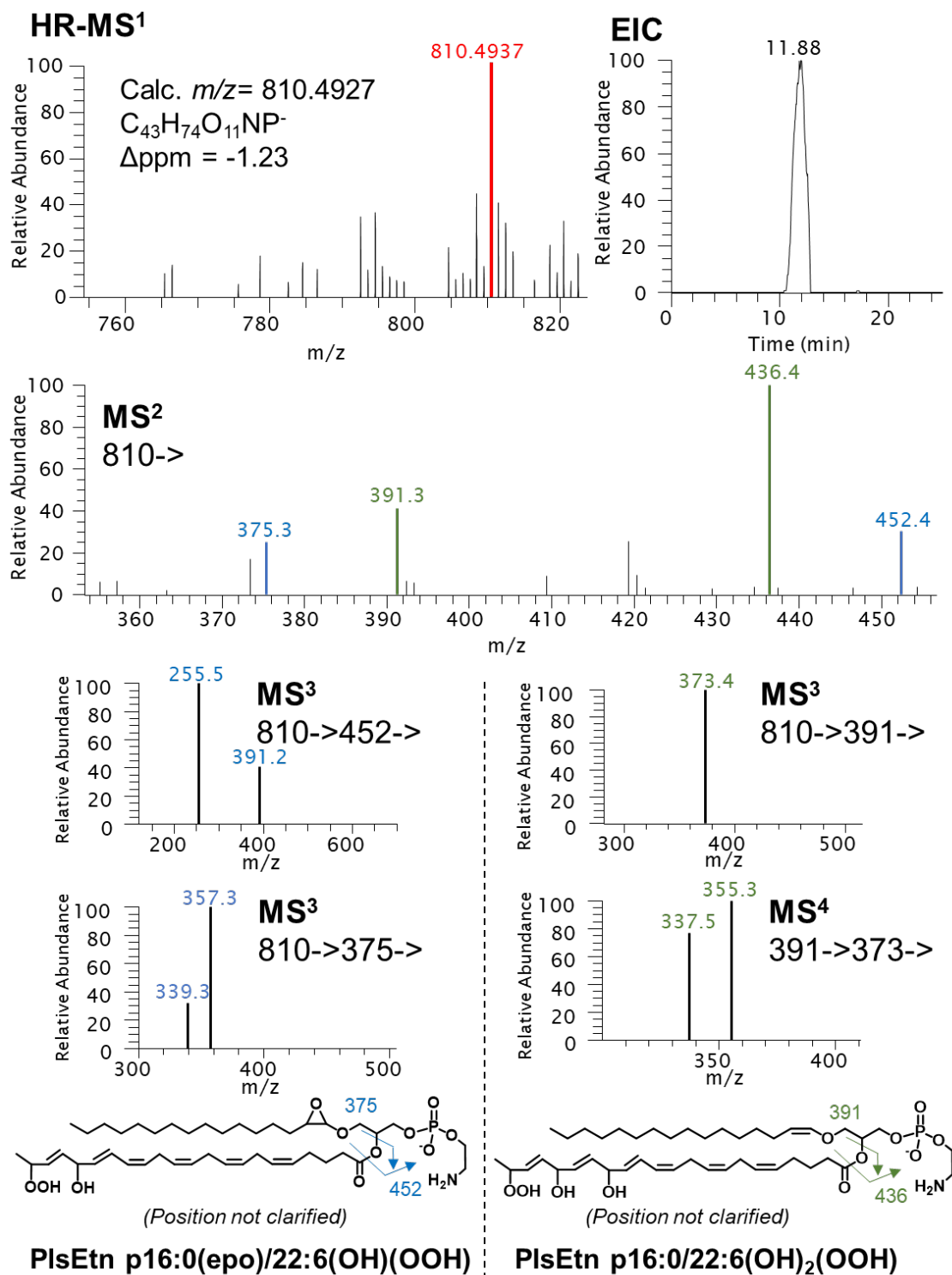


Figure S4. Identification of PlsEtn 38:6+4[O] by HR-MS and tandem MS.

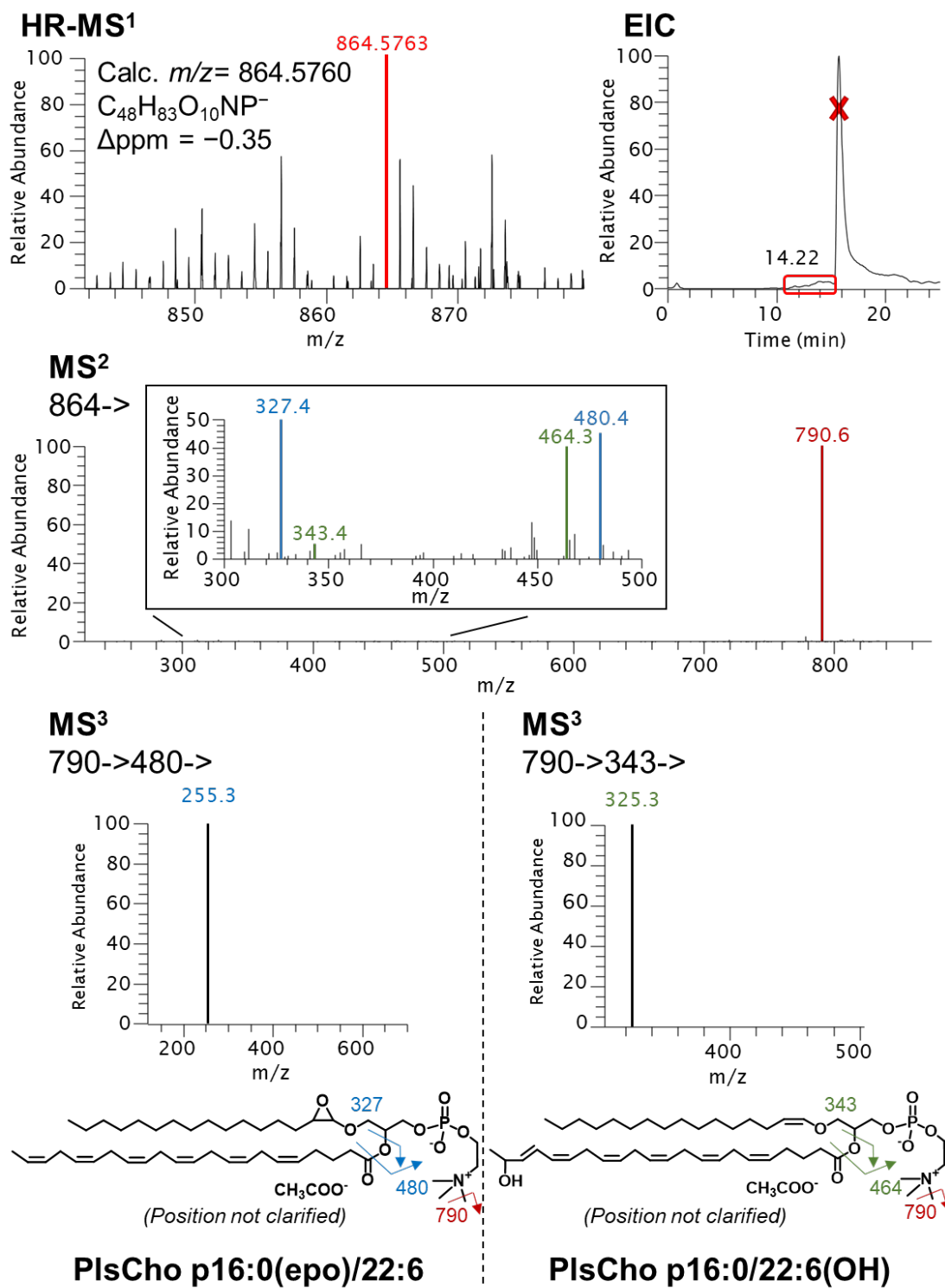


Figure S5. Identification of PlsCho 38:6+1[O] by HR-MS and tandem MS.

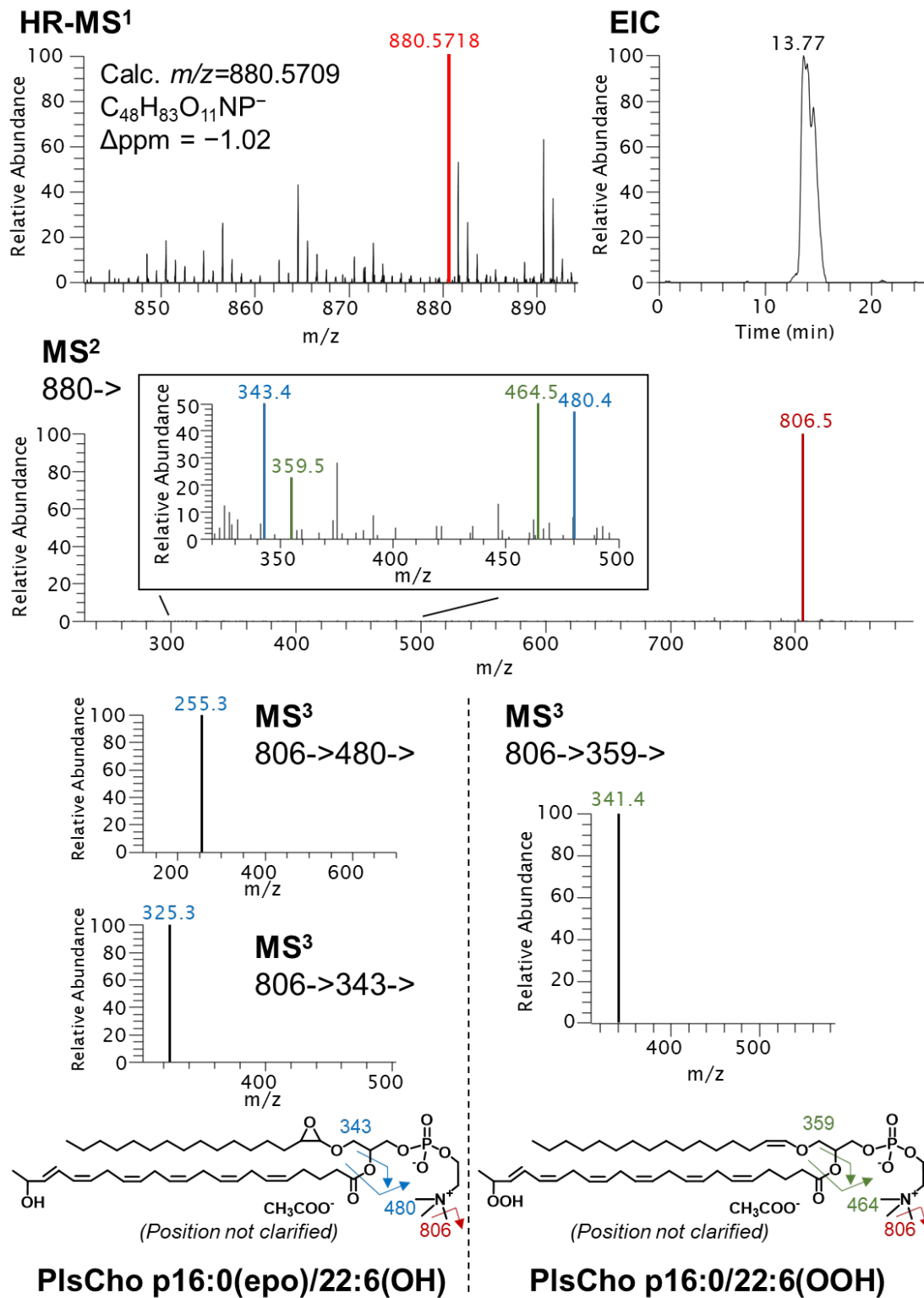


Figure S6. Identification of PlsCho 38:6+2[O] by HR-MS and tandem MS.

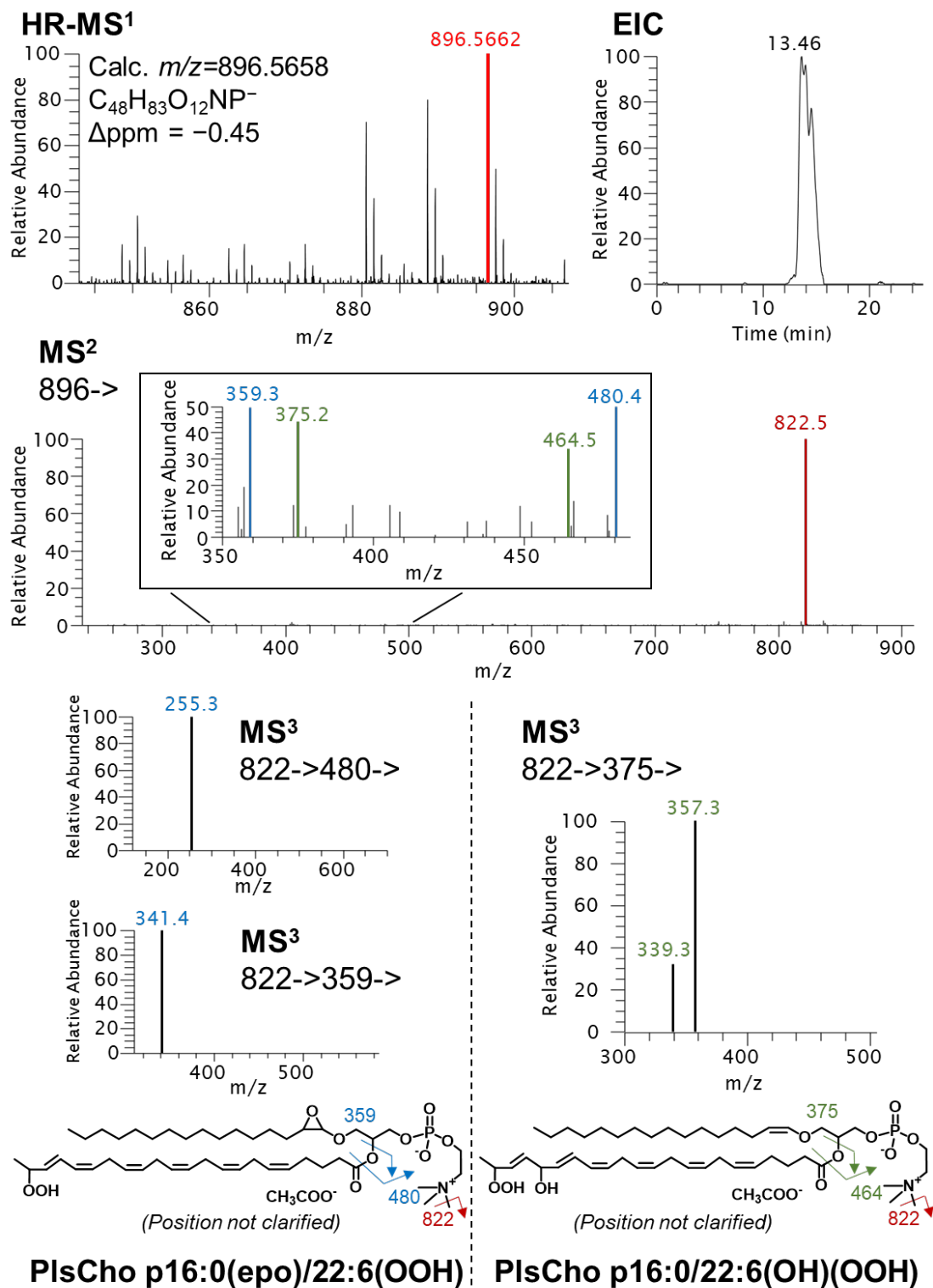


Figure S7. Identification of PlsCho 38:6+3[O] by HR-MS and tandem MS.

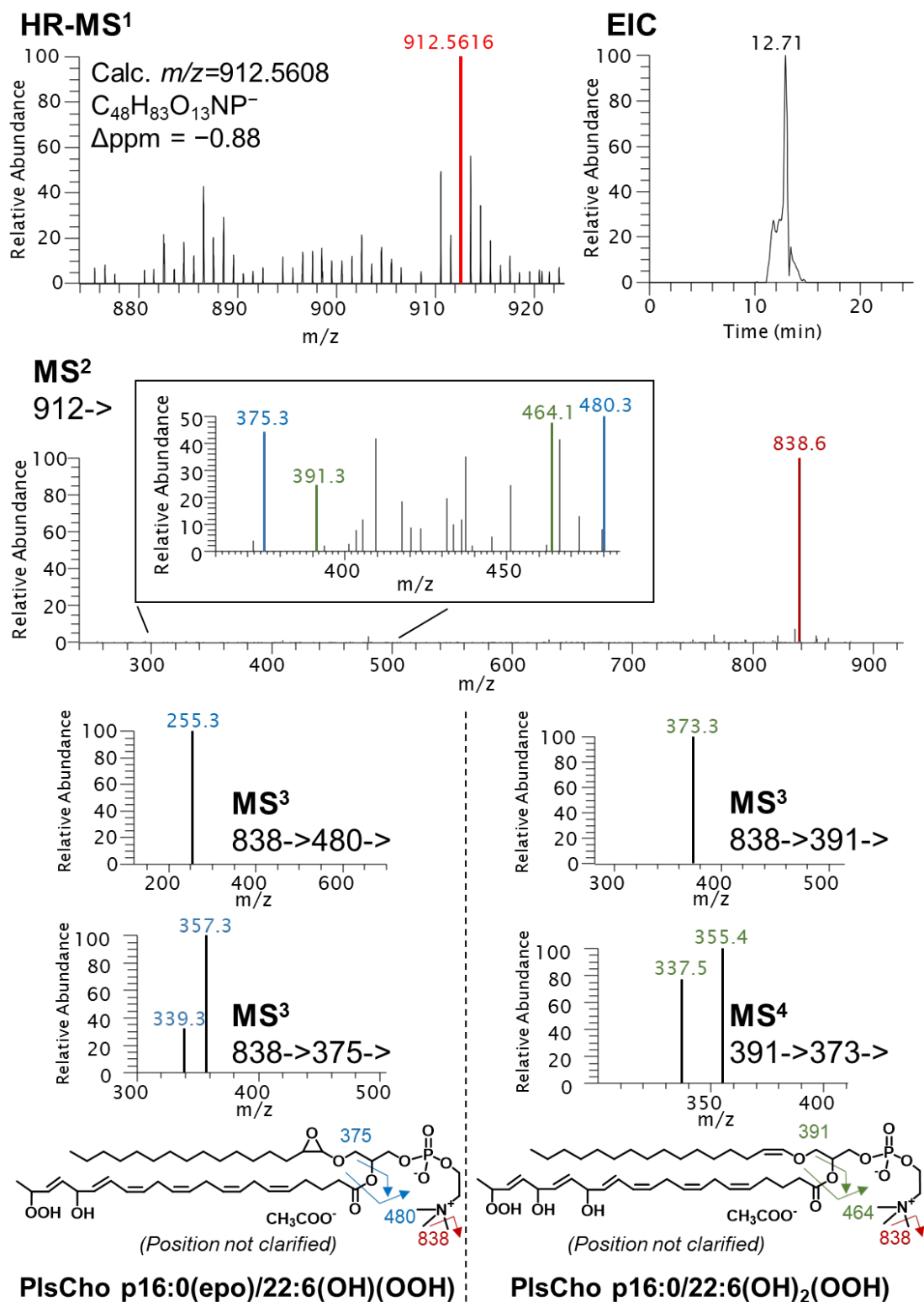


Figure S8. Identification of PlsCho 38:6+4[O] by HR-MS and tandem MS.

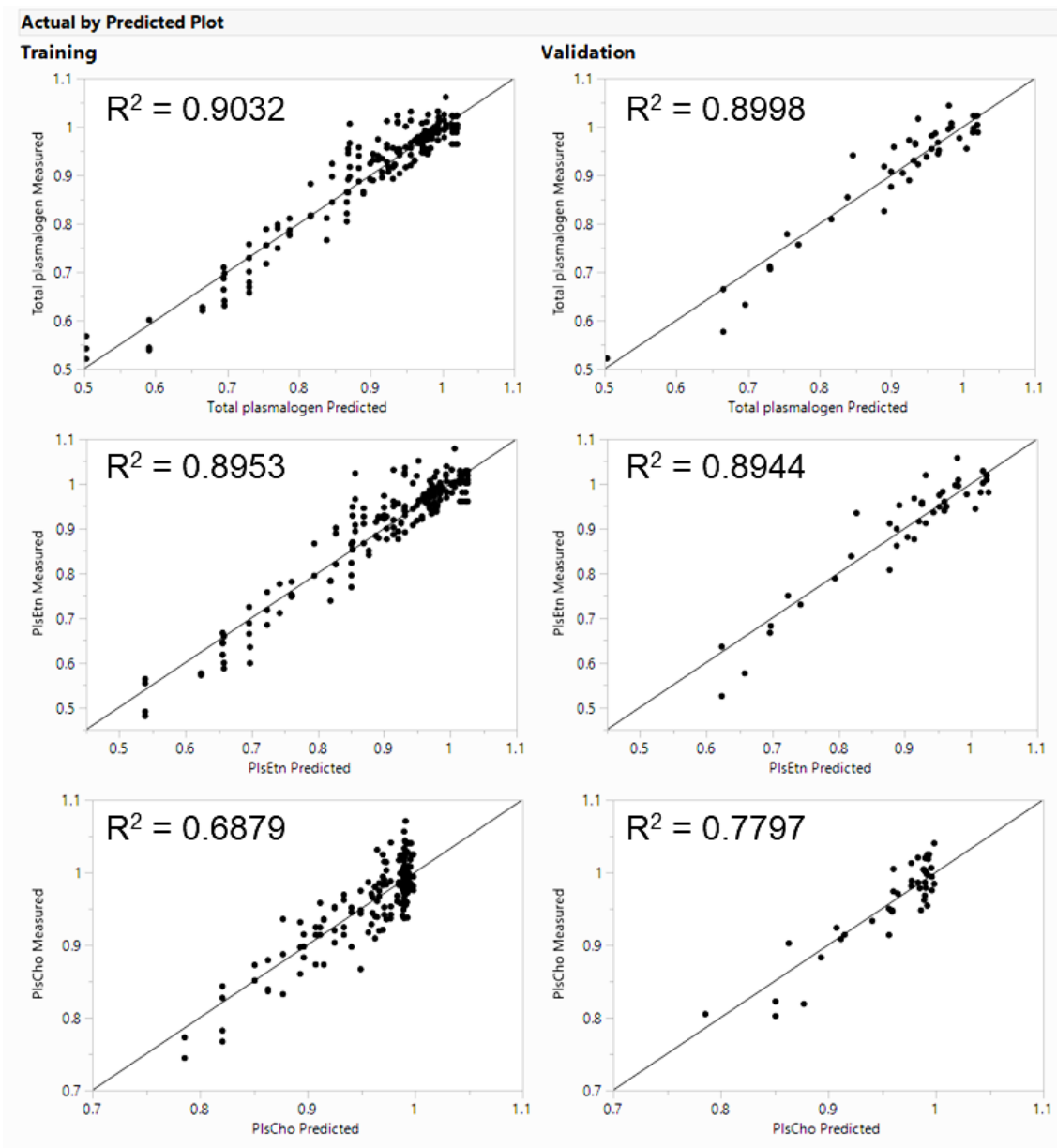
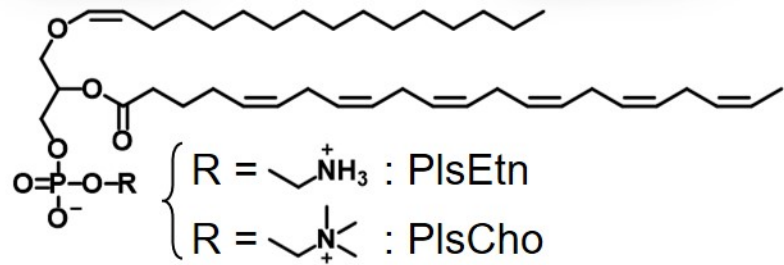
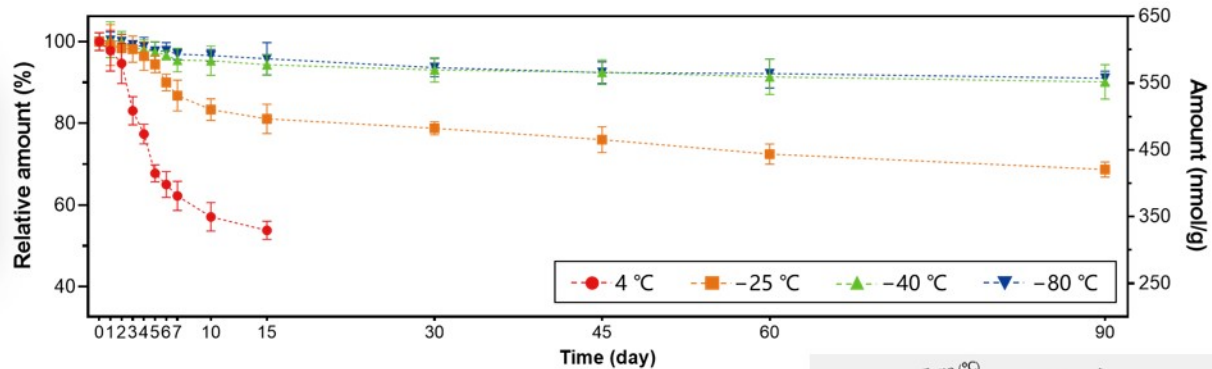


Figure S9. Measured vs. predicted values in training and validation data set for the remained content of the plasmalogen species during storage.



Plasmalogens  $\begin{cases} \rightarrow \text{Oxidation} \\ \rightarrow \text{Degradation} \end{cases}$

